CENTRO DE INVESTIGACIÓN Y DE ESTUDIOS AVANZADOS DEL INSTITUTO POLITÉCNICO NACIONAL

Unidad Mérida
DEPARTAMENTO DE FÍSICA APLICADA

"Estudio experimental del oscilador electroquímico cadmio/cianuro"

TESIS

Que presenta

Daniel Arcángel López Sauri

Para obtener el grado de

Doctor en Ciencias

En

Fisicoquímica

Director de Tesis:

Dra. Lucien Veleva Muleshkova

Mérida, Yucatán, México marzo de 2016

CENTRO DE INVESTIGACIÓN Y DE ESTUDIOS AVANZADOS DEL INSTITUTO POLITÉCNICO NACIONAL

Unidad Mérida
DEPARTAMENTO DE FÍSICA APLICADA

"Experimental study of the cadmium/cyanide electrochemical oscillator"

Thesis presented by:

Daniel Arcángel López Sauri

To obtain the degree of

Doctor of Sciences

In

Physical Chemistry

Thesis Director:

Dra. Lucien Veleva Muleshkova

Mérida, Yucatán, México marzo de 2016

ACKNOWLEDGMENTS

I would like to thank the National Council for Science and Technology of México (CONACYT), for the financial support given to the realization of this postgraduate program, as well as the Research Center and advanced studies of I.P.N (CINVESTAV), for receiving me as one of their students and for all their support during these four years, not only during my stay in the Center but also for the financial support for attendance at conferences.

This thesis would not have been possible without the generous assistance of Dr. Lucien Veleva, my thesis adviser, who guided me through this path. I also would like to thanks to Dr. Gabriel Pérez for his support and advices on topics of nonlinear dynamics. I appreciate the comments of my Synod: Dra. María Cebada, Dra. Patricia Quintana and Dr. Luis Díaz. I also want to thank you for letting my defense be an enjoyable moment, and for your brilliant comments and suggestions, thanks to you.

A special thanks to my family. Words cannot express how grateful I am to my mother and father for all of the sacrifices that you've made on my behalf. Your prayers for me were what sustained me thus far. I would also like to thank all of my friends, who supported me during these years.

RESUMEN

En experimentos bajo condiciones potentiostaticas y galvanostáticas se observaron oscilaciones de corriente y potencial catódicas durante el electrodepósito de cadmio a partir de un electrolito de cianuro sobre un electrodo vertical de platino, en soluciones con diferentes relaciones de concentración de Cd^{2+}/CN^{-}. Experimentos de espectroscopía de impedancia electroquímica (EIS por sus siglas en inglés) revelaron una región de impedancia real negativa en un rango de frecuencias diferentes de cero, en la meseta de la curva de corriente-potencial con forma de N. Este tipo de comportamiento dinámico es característico de los osciladores electroquímicos HN-NDR (por sus siglas en inglés), estos osciladores presentan curvas de corriente-potencial con forma de N y una resistencia diferencial negativa oculta. Las oscilaciones pueden ser atribuidas a los cambios en el área catódica activa del electrodo, debido a la adsorción de moléculas de hidrógeno y su desprendimiento desde la superficie. Las inestabilidades del proceso electroquímico se caracterizaron por series de tiempo, transformadas rápidas de Fourier y diagramas de fase en 2-D mostrando oscilaciones con un comportamiento cuasi-periódico y caótico, dependiendo de las condiciones experimentales.

ABSTRACT

Cathodic current and potential oscillations were observed during electrodeposition of cadmium from a cyanide electrolyte on a vertical platinum electrode, in potentiostatic and galvanostatic experiments, from solutions with different Cd^{2+}/CN^{-} concentration ratios. Electrochemical impedance spectroscopy (EIS) experiments revealed a region of negative real impedance in a range of non-zero frequencies, in the plateau branch of the N-Shape current-potential curve. This type of dynamical behaviour characterises the HN-NDR electrochemical oscillators, these oscillators display N-Shape current-potential curves and a Hidden Negative Differential Resistance (HN-NDR). The oscillations could be mainly attributed to changes on the electrode's active cathodic area, due to the adsorption of hydrogen molecules and their detachment from the surface. The instabilities of the electrochemical processes were characterized by time series, Fast Fourier Transforms and 2-D phase portraits showing quasi-periodic and chaotic oscillations, depending on the experimental conditions.

CONTENTS

Chapter 1

Introduction

1. A BRIEF INTRODUCTION TO NON-EQUILIBRIUM PHENOMENA IN ELECTROCHEMISTRY

The world is a dynamical system and this system is mostly nonlinear. Many phenomena which we experience in everyday life, not only in research laboratories, are nonlinear in their dynamics. This behaviour is more evident in periodic phenomena occurring in living organisms, such as leaf colour changes or heartbeat rhythms, and in pattern formation in biological and certain geological systems. Nonlinear behaviour has produced great interest across the world chemistry community [1].

Fig. 1 Examples of nonlinear phenomena in nature and living organisms

Modern nonlinear chemical dynamics was started around the 50's by Boris Pavlovich Belousov [2-8]. Belousov observed periodic changes in colour during the oxidation of an organic substrate, such as malonic acid, by acidified bromate catalized by a redox couple of cerium ions. Belousov had difficulty in publishing his results, but they were finally brought to the attention of Western chemists by Anatoly Zhabotinsky, who was more successful in popularizing the reaction, which today is known as the Belousov-Zhabotinsky (BZ) reaction and has played an important role in nonlinear chemical dynamics, similarly to the hydrogen atom in quantum mechanics [9].

Electrochemical reactions have many types of dynamical behaviour, which make their use in dynamics studies very interesting. Non-steady behaviour during electrochemical experiments can be dated back to 1828 [10], and has been the subject of numerous investigations since that time. In fact, there are probably more examples of oscillating systems in electrochemistry than in any other branch of chemistry [11-43]. It is important to note that their dynamics display striking analogies, when compared with other types of dynamical systems, like chemical [44], physical [45], and biological ones [46], and even in phenomena occurring in the stock market [47]. Since each of these categories deals with its specific language, the universalities in the dynamical behaviours manifest themselves clearly only at the level of mathematical description, which in turn is based on the behaviour of solutions of nonlinear differential equations. Therefore, nonlinear dynamics is really an interdisciplinary science.

When maintained far from thermodynamic equilibrium, chemical reacting systems can exhibit a rich variety of spatio-temporal self-organization, if they are governed by the appropriate nonlinear evolution laws. The most common way in which such a self-organization manifests itself, is through the occurrence of spontaneous reaction-rate oscillations [48].

Electrochemical oscillations can be easily monitored by simple current, potential, or voltage control, and parametric changes of a few orders of magnitude can be easily applied. Nonlinear electrochemical systems have been found to be most valuable as models for more complicated chemical or physiological nonlinear systems, because of their similarities, for example as models for information transfer in mammals [49] or in stimulus-response behaviour analogous to that of a nerve [46].

Electrochemical oscillators were proposed as model systems for nerve impulse propagation and have been shown to possess the characteristic dynamical features of simple neurons. Similarly to biological neurons, the electrical potential or the current are the oscillating quantities. Besides this similarity, electrochemical oscillators constitute the most suitable 'artificial neurons' in oscillatory associative memories (AM) [50]. An associative memory is a device that can store prototype patterns and recall them together with their associated attributes, even from distorted or incomplete input information. The way in which data are stored and retrieved in an AM and in a digital computer is fundamentally different. In digital computers, data are accessed when their correct binary addresses in memory are given. By contrast, in an AM, the data words are accessed based on the whole content of the input pattern. The entire mapping of the input to output patterns is distributed in the AM without storage location implemented through dense connections. This property makes AMs error-tolerant and capable of learning. The units or neurons of conventional neurocomputers or artificial neural nets are highly interconnected; if the number of neurons is n, the net possesses n^2 connections. The high degree of interconnectivity and the need to adjust the strength of the interconnections in the learning process constitute major obstacles in realizing corresponding hardware. Associative memories that are based on globally coupled nonlinear oscillators operate qualitatively different. The simplest type of oscillatory neurocomputers needs only n connections because the n oscillators have only a single connection to a common support. Then, the learning process involves a single global coupling element; the pattern being encoded is the time-dependent external input to the global coupling element. The only requirement is that the frequencies of the n oscillators can vary significantly.

The variation of a parameter in electrochemical systems, such as voltage or current, can change the behaviour from steady to oscillatory; with further variation a simple periodic oscillation can change to one with twice the period or can change to an oscillation with two fundamental incommensurate frequencies (quasiperiodicity) or even to a more complicated behaviour like chaos [11].

The majority of electrochemical systems, for which oscillations and other interesting dynamics have been reported, involve the anodic dissolutions of various metals [12-23], oxidation [24-28] or reduction of molecules [29-31]. Only a few papers report on

oscillations during electrodeposition processes and most of them are focused on galvanostatic potential oscillations, like those during the electrodeposition of Sn [32], Cu/CuO layered structures [33, 35], Cd [36] and Ag-Cd alloys [37]. Potentiostatic current oscillations have been found during electrodeposition of Ni [38], Cu-containing imidazolium ionic liquids [39], In [40] and Cu-Sn alloys [41-43]. Figure 2 shows examples of oscillations in electrochemical systems.

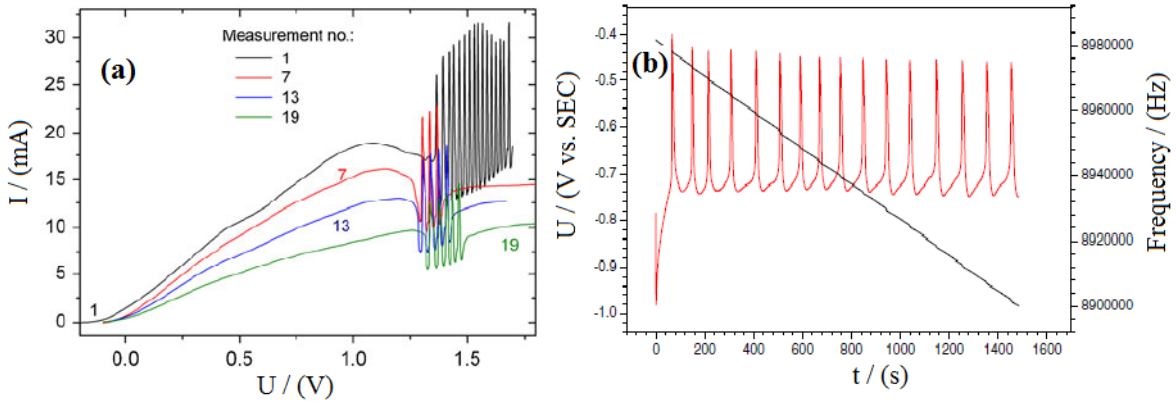

Fig. 2 (a) Current oscillations in the current-potential curves for a sequence of anodic polarization on stationary vanadium electrode (taken from ref. [12]), (b) potential oscillations during electrodeposition of layer of Cu and Cu_2O in alkaline citrate solutions and EQCM response obtained under galvanostatic conditions (taken from ref. [34]).

The theoretical behaviour and classification strategies for oscillating electrochemical processes, based on electrochemical impedance spectroscopy (EIS) and the kinetic nature of negative faradaic impedance, are described in several papers by Koper *et al.* [51-61].The electrochemical oscillations were classified depending on whether the steady-state current-voltage exhibits (i) a negative slope with a negative impedance, or (ii) a positive slope with a "hidden" negative impedance. Even a negative impedance is not apparently indispensable for the onset of the oscillations [57]. The distinction of the four principal oscillator categories refers to the mechanistic role of the double layer potential in the presence of at least one autocatalytic variable [60, 61], that is, either a chemical species or an electrical quantity.

-Class I is given by strictly potentiostatic oscillators, where the potential is non essential, while both the autocatalysis and the slow species are purely chemical.

-Class II has S-shaped voltammetric curves, where the potential is the essential slow variable with the autocatalysis still chemical.

-Classes III and IV, are those where the potential is autocatalytic, with a chemical species forming the slow, negative feedback. Despite the common features, both categories exhibit distinct dynamical behaviour. Class III exhibits a negative real impedance in combination with a region of negative slope in their steady-state current-voltage curve, and it is referred to as "NDR oscillators", because of the indispensable presence of the negative differential resistance. Class IV has a "hidden" negative impedance, coupling with a positive slope in the steady-state current-voltage curve, and they are called "HNDR oscillators".

Even if these principal four classes represent a complete classification scheme, it is not excluded that the introduction of further subcategories may become appropriate in the future, because of the new electrochemical oscillators, discovered with different oscillatory mechanisms [62, 63].

The model based on the concept of additional current carrier (current gives rise to a reaction involving charge transfer) originated an interesting discussion in the literature on the role of convection in the onset of electrochemical instabilities. For example, iodate reduction with N-shape current-potential relationship, due to a Frumkin repulsive effect (variation of potential in the double-layer region, e.g. repulsive interaction of ions with the charged electrode surface) and hydrogen evolution, as an additional current carrier, are emphasized in the NDR-based model [59], without considering the convection mass transfer. An alternative explanation also involves hydrogen evolution as a process crucial for the onset of instabilities, as a source of convection [64-68].

Li *et al.* have suggested that electroreduction of $Fe(CN)_6^{3-}$ on a Pt electrode presents bistability (two coexisting stable steady states) coupled with convection feedback induced by hydrogen evolution [65], which accounts for the potential oscillations. The authors have proposed a mechanism of galvanostatic potential oscillations, which should operate in the region of diffusion-limited current plateau [64-68]. As long as the current originating from a primary electrode process equals the imposed current, the electrode potential is stable. However, continuous depletion of the diffusion layer, caused by the electrode process and relatively slow diffusion, is the reason for a continuous decrease of a faradaic current, shifting the electrode to a more negative potential (for cathodic processes), at which the additional process, that is hydrogen evolution, takes place. The resulting detached bubbles of hydrogen cause the sudden convection, which replenishes the surface concentration of

the primary reactant, and the current rises again above the diffusion-limited plateau, causing the return of the electrode potential to less negative values.

Galvanostatic potential oscillations during electrodeposition of cadmium from alkaline electrolytes have been reported by Kaneko *et al*. [36]. Kaneko suggested that when the electrolysis was carried out at current densities above the limiting one, hydrogen evolution occurs, acting as the principal source of convection. Vishomirskis [69] suggested that the reason for the galvanostatic potential oscillations is the formation/destruction of some passive film, formed on the surface of the electrode, and that hydrogen evolution does not play the main role originating the oscillations.

X-ray photoelectron spectroscopy (XPS) investigations confirmed the existence of passive films at potentials corresponding to the onset of oscillations, which, besides the hydrogen evolution under limiting current density, could be an additional promoter of the system's oscillatory behaviour [70].

Many electrochemists have been fascinated by periodic electrochemical reactions, trying to obtain the explanation of the origin of such oscillatory phenomena [10-43, 48-85].

2. SCOPE AND OUTLINE

The aim of this thesis is to apply the concepts of electrochemical reactions under far-from-equilibrium conditions to the study of the oscillatory behaviour observed in the cadmium/cyanide system. The origin of the instabilities during the cadmium electrodeposition from cyanide electrolytes onto platinum electrodes will be studied within the framework of the classification of electrochemical oscillators. The registered time series of the oscillations at galvanostatic and potentiostatic conditions are analyzed by the Fast Fourier Transform (FFT) and space phase projections, to study their behaviour.

Chapter 2 introduces the concept of systems far-from-equilibrium, and how it is related with electrochemical systems. A summary of stability in electrochemical systems, and its relationship with the Electrochemical Impedance Spectroscopy Technique, for the classification of electrochemical oscillators, is discussed. In chapter 3, we will turn our attention in the nonlinear behaviour of cadmium electrodeposition, which is the principal subject of the present thesis.

Chapter 2

Instabilities in far-from-equilibrium electrochemical systems and their classification

1. FAR-FROM-EQUILIBRIUM SYSTEMS

When maintained far from equilibrium and open to exchange of energy and/or matter with their surroundings, nonlinear chemical systems are able to self-organize taking on ordered states of locally decreased entropy such as temporally periodic, chaotic, or spatially periodic variations of concentrations of chemical species [44]. Because of the seemingly tight grip of the second law of thermodynamics, periodic phenomena in chemistry were not accepted as reality or at best considered mere laboratory curiosities throughout the 19th and much of last century.

Classical thermodynamics deals with equilibrium states, but tells us very little about how the equilibrium is reached and nothing about how a system will behave when it is maintained far from equilibrium permanently, and many scientists have been led astray to the assumption that equilibrium is reached in a simple way and that a constant thermodynamic force applied to a system will simply result in a constant thermodynamic flow [71].

Spontaneous oscillations around equilibrium, in fact, would require both the Gibbs free energy and the entropy to oscillate, thereby violating the second law. Finally, the advent of non-equilibrium thermodynamics in the non-linear regime [72] and the concept of dissipative structures would resolve the dilemma [73]. Simultaneously, enhanced dissipation of energy through the system to the surroundings assures a net increase of entropy in accordance with the second law. Stopping the exchange of energy and matter, the system gradually approaches chemical equilibrium until all patterns cease. The requirements for an oscillating reaction to occur are classified in thermodynamic and kinetic. The thermodynamics demands that the system is far from equilibrium, i.e. The

Gibbs free energy of the overall reaction is large and negative. The minimum kinetic condition requires a nonlinear dynamic mass law [1-4]. Electrochemical kinetics is inherently nonlinear, and electrochemical experiments are usually performed far from equilibrium. It is only under these conditions that the possibility of non-equilibrium instability arises: the thermodynamic branch loses its stability and will give way to a new and in many cases, more organized state. This tendency of non-equilibrium systems to self-organize can express itself in the form of temporal periodicities (spontaneous oscillations) or spatial periodicities (spatial structuring) [71].

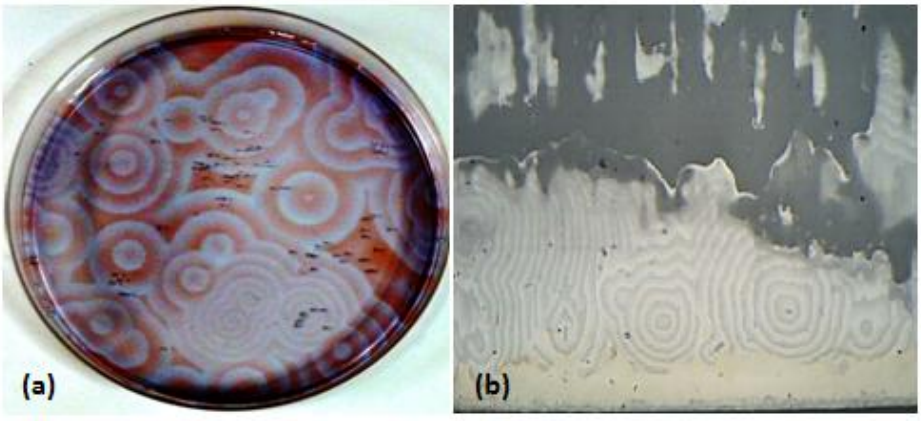

Fig. 3 Comparison of spatial structuring: a) in the chemical oscillator of Belousov-Zhabotinsky, and b) during electrodeposition of Ag-In alloys (taken from ref. [74]).

Mathematically, dynamical systems are defined in terms of differential equations which can be of two types, ordinary if the dynamic variables depend solely on time, or partial if the variables depend also on the spatial coordinates. Let us assume that the differential equations meeting all the conditions at which self-organization occurs were formulated in terms of appropriate dynamic variables, i.e. intermediate concentrations, electrode potential, etc. The occurrence of self-organization, e.g. spontaneous oscillations of these variables, depends now on the values of parameters (control parameters) that are included in these equations, for example, the applied electrode potential or electric current imposed for electrochemical processes. It may happen that for some control parameters which we choose initially, the solutions of those equations will be quite trivial, predicting the existence of only a single steady state. However, for another set of those parameters the same equations may generate spontaneous temporal oscillations of the variables [60, 62, 71-73, 75, 76]. Under certain conditions these nonlinear equations can themselves exhibit

chaotic properties. In order to distinguish this feature from the entropic chaos of the equilibrium, and to underline the deterministic origin of these aperiodicities, this kind of chaos in referred to as deterministic chaos. [1-5, 62, 71].

2. FAR-FROM-EQUILIBRIUM PHENOMENA IN ELECTROCHEMICAL SYSTEMS

Electrochemistry has always been related to the assessment of what determines the kinetics of redox reactions at electrode/electrolyte interfaces, in finding out what happens during corrosion or deposition processes, but many of such studies are based on the assumption that the electrochemical reaction rate (the faradaic current) possesses a well-defined and accessible steady state. Nature does not always behave as simply as we would like it to, and the occurrence of spontaneous reaction-rate oscillations have been observed in a wide variety of electrochemical systems [71].

Oscillations and surface patterns can arise in electrochemical reactions. In potentiostatic (constant potential) systems the current can oscillate and in galvanostatic (constant current) systems the potential can oscillate, displaying simple or complex periodic, quasiperiodic or chaotic oscillations [11]. For many years, researchers have ignored such behaviour, assuming it was difficult to explain, because it involves the solution of nonlinear differential equations, which require in practice a numerical approach using digital simulations on a computer.

In 1828, Fechner reported for the first time an oscillatory behaviour in an electrochemical system, when he observed periodic oscillations during electrodissolution of iron in an acidic silver nitrate solution [10], and this kind of behaviour has been the subject of numerous investigations since then.

Electrochemical systems, for which oscillations and other interesting dynamics have been reported, involve the anodic dissolutions of various metals [12-23], oxidation [24-28] or reduction of molecules [29-31], galvanostatic electrodeposition [32-37] and potentiostatic electrodeposition [38-43] of metals. A recent review by Hudson and Tsotsis [11] contains about 500 references of electrochemical reaction dynamics, being probably a small percentage of what has been published in the literature.

For many years, electrochemists have been fascinated by periodic electrochemical reactions, and started to involve nonlinear dynamic tools to explain them. Studying dynamic behaviours in electrochemistry has some advantages over similar investigations in other fields of chemical kinetics. For example, electrochemical experiments require a relatively simple and cheap equipment (a potentiostat/galvanostat), with which the external control and the displacement out of the thermodynamical equilibrium is easily established, as it suffices to apply a potential different from the equilibrium potential or a current different to zero. Additionally, the time scale of electrochemical oscillations is relatively short (in the range of milliseconds to seconds), as compared to other chemical oscillators, allowing a rapid acquisition of data [71].

The application of nonlinear dynamics in the origin of the instabilities appears to be useful to describe the different mechanisms of the oscillatory phenomena, not only in electrochemical oscillators, but also in materials science [75, 76].

3. STABILITY IN ELECTROCHEMICAL SYSTEMS

Nonlinear chemical reactions systems, which operate far from equilibrium, can exhibit a rich variety of dynamic states other than a single stationary state (monostability). When non-equilibrium system switches from one type of dynamics to a qualitatively different one, as one or more control parameters (externally applied potential, bulk concentrations or temperature) are varied, it is called bifurcation. In this respect, non-equilibrium bifurcations are very much like phase transitions in an equilibrium system. From concepts of nonlinear systems theory, dynamic states can be classified according to their complexity. The simplest instability involves two coexisting stable steady states for a given set of control parameters (bistability). This transition between mono- and bistability is referred to as saddle-node (sn) bifurcation, and it gives rise to hysteresis behaviour in current/potential curves. Spontaneous oscillations in physico-chemical systems are generally related to the steady state, becoming unstable in favour of a periodic orbit [76]. The transition point is referred to as Hopf (h) bifurcation; finally, another transition can lead to unstable periodic orbits and can result in complex chemical dynamics such as deterministic chaos [77].

If we consider a simple electrochemical cell, consisting of two electrodes: the polarisable working electrode and an ideally non-polarisable reference electrode; all the resistances exhibited by the system will be summarized to a single value of an equivalent resistance R_s, which is connected in series with the cell [62]. We apply a sufficiently high external voltage (U), which will compensate the own electromotive force of the cell and polarise the working electrode to the value at which the faradaic current flows at the working electrode. In consequence, the electric current flows through the entire circuit. This situation can be represented in Fig. 4 in terms of its equivalent circuit, which consists of a resistor (linear element) and the electrolytic cell (non linear element), symbolized by a box with cross. The nonlinear current-potential dependence on the electrode process in this cell is denoted further as $I_2(E)$.

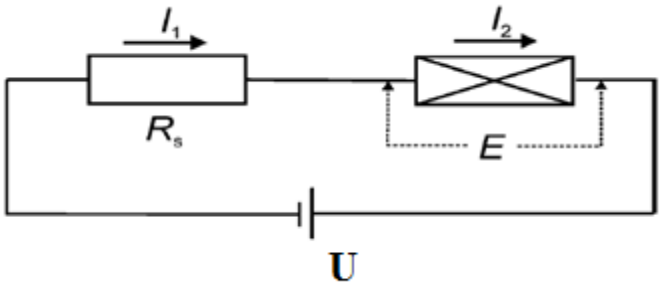

Fig. 4 Simplified equivalent circuit of the electrochemical system consisting of electrolytic cell and power source, with all resistances summarized into an equivalent ohmic resistance R_s (taken from ref. [62]).

In the steady-state both currents are equal: $I_1=I_2$, so there is no increasing accumulation of electric charge at the working electrode-solution interface ($dE/dt=0$). Beyond the steady-state, the electrode potential E changes according to the dependence:

$$\frac{dE}{dt} \propto (I_1 - I_2) \tag{1}$$

Irrespective of that, whether the system is actually in steady-state or not, current I_1 is given by:

$$I_1 = \frac{U-E}{R_s} = \frac{U}{R_s} - \frac{E}{R_s} \tag{2}$$

where E means the potential drop at the working electrode/solution interface (interfacial potential drop). The dependence (equation 2) is known as the equation of the load line, representing the response of a linear circuit connected to the nonlinear device [62]. It is thus

a straight line in the *I–E* coordinates, with the intercept U/R_s and the slope $-1/R_s$. In terms of such representation it is clear that the steady-state(s) of the circuit from Fig. 4 (E_s, I_s) is (are) determined by the intersection(s) of a load line with the $I_2(E)$ characteristics of the electrode process: i.e., when $I_1(E_s)=I_2(E_s)$. The analysis of stability/instability of these steady-states, crucial for diagnosis of possible dynamic regimes under different conditions, is described below.

3.1. Stability of the N-NDR System under potentiostatic control

Let us assume that external voltage *U* is constant, which means here the potentiostatic conditions applied to the whole circuit. Note that here this term has a different sense that in classical electrochemistry, where the term "potentiostatic" usually means constant working electrode potential *E*, due to minimization (compensation) of the serial resistance, and thus of the ohmic drops. From the point of view of possible dynamic instabilities these two cases are fundamentally different. In order to distinguish between them, the case of constant *E* will be called the "truly potentiostatic condition", according to the literature about electrochemical instabilities [48, 60-62].

Returning to the case of *U*=constant, according to Eq. (2), any change in I_1 (e.g., due to fluctuation) will cause the appropriate change in *E*, the higher the change in *E* the greater the serial resistance: $dE = -R_s(dI_1)$. The response of the electrode potential *E* to this perturbation (its evolution in time) will indicate whether the perturbed steady-state is stable or not. This depends on the kinetic characteristics $I_2(E)$ of the electrode process. Based on Eq. (1), the stability of the steady-state is given by the sign of the derivative $d(dE/dt)/dE$, which is proportional to the difference in the slopes of $dI_1(E)/dE$ and $dI_2(E)/dE$:

$$\frac{d}{dE}\left(\frac{dE}{dt}\right) \propto \left(\frac{dI_1}{dE} - \frac{dI_2}{dE}\right) \tag{3}$$

This means that the direction of the temporal variation of the electrode potential depends on the relation between the charging and discharging of the electrode.

The considered electrochemical system is unstable with respect to perturbation *dE*, if:

$$\frac{d}{dE}\left(\frac{dE}{dt}\right) > 0 \tag{4}$$

From Eq. (2), the slope dI_1/dE is always negative:

$$\frac{dI_1}{dE} = -\frac{1}{R_S} \tag{5}$$

So, in view of Eq. (3), the instability condition (Eq. (4)) requires that:

$$\frac{dI_2}{dE} < -\frac{1}{R_S} \tag{6}$$

As a simple linear element the serial resistance R_s cannot be negative; so the slope dI_2/dE must be negative. This derivation leads us to the first important instability condition: *simple electrochemical systems, characterized by one dynamical variable, the electrode potential E, will be unstable provided there is a region of negative differential resistance (NDR) in its current-potential characteristics* [62]. The second condition is that the serial resistance must be sufficiently high, as the condition of Eq. (6) is equivalent to:

$$R_S > -\frac{dE}{dI_2} \equiv -NDR \tag{7}$$

A graphical illustration of the condition of instability is presented in Figure 5. The N-shape I_2-E curve (meaning the N-NDR type of characteristics), which is recorded under truly potentiostatic conditions, gives rise to the region of negative dI_2/dE slope.

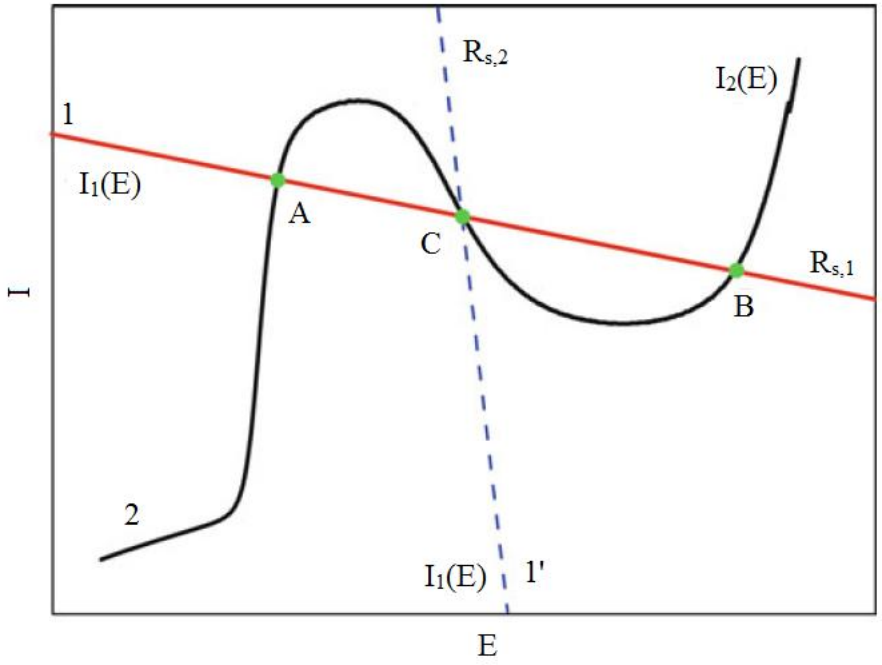

Fig. 5 Graphical illustration of the principle of determination of stability of the steady-states for the electrode process characterized with the N-shape negative differential (N-NDR) region (curve 2) for the load lines corresponding to serial resistance: $R_{s,1}$ (line 1) and $R_{s,2}$ (line 1'), with $R_{s,1}>R_{s,2}$ (taken from ref. [62]).

The I_2-E dependence is intersected by two examples of linear load lines, of different slopes, corresponding to two serial resistances $R_{s,1}$ and $R_{s,2}$, with $R_{s,1}>R_{s,2}$. It is possible to conclude [62]:

1) When the serial resistance R_s is zero, then the load lines 1 and 1' with finite slopes and intercepts do not exist. Therefore, the electrode potential E is equal to the external voltage U and the entire N-shape, steady-state dependence I_2-E can be experimentally recorded, point by point, under truly potentiostatic conditions, that means, all the states composing the I_2-E dependence are stable under truly potentiostatic conditions (to every value of E, only a single value of steady-state current corresponds), otherwise they would not be directly detectable.

2) If a non-zero (positive) serial resistance R_s is inserted in the circuit of Fig. 4, the electrode potential E and external voltage U become different in the presence of current. A load line appears on the diagram, with the intercept equal to U/R_s and the slope equal to $-1/R_s$. The number and stability of steady-states possible for a given (U, R_s) parameters is now indicated by the intersections of the load line I_1-E with the I_2-E curve of the electrochemical system.

3) When the serial resistance is sufficiently small ($R_{s,2}$), only one intersection exits (C) of these two characteristics; for a given external voltage U there is only one steady-state possible, which is stable against perturbations, in spite of lying on the NDR branch of the system's characteristics. Therefore, the system is monostable.

4) If the serial resistance is so high that the condition of Eq. (7) is met, for the corresponding (U, R_s) parameters three steady-states (A, B, C) are possible, of which external ones (A, B) are stable, while the middle one (C), the only one lying on the NDR branch, is now unstable. This case corresponds to bistability, i.e., for a given U the system can exist either in state A or B, belonging to the upper (A) and lower (B) branch of the folded diagram of states. The transition between the monostable and bistable behaviours is associated with the saddle-node bifurcations, occurring twice when the condition $R_s = -\mathrm{d}E/\mathrm{d}I_2$ is met: once when the system enters the bistable region and a second time when the system leaves it upon continuous variation of external voltage U.

5) All steady-states belonging to the N-NDR region of the truly potentiostatic I_2-E dependence can become unstable under potentiostatic (U constant) conditions, provided

sufficiently high resistance R_s is present in the circuit. This resistance cannot be too high (for a given voltage U) since then the load line may not penetrate the NDR region and the system returns to monostable behaviour.

3.2. Stability of the N-NDR system under galvanostatic control

The galvanostatic mode does not mean the absence of a serial resistance: the switching from potentiostatic to galvanostatic mode can be interpreted as the insertion of the (theoretically) infinitely high serial resistance R_s, to which an (theoretically) infinitely high voltage U is applied, with the U/R_s ratio defining the imposed current. Then, even if the resistance of the electrochemical cell r (with $r << R_s$) varies as a function of, e.g., changing electrode potential, the current which flows through the entire circuit remains practically the same: $U/(R_s + r) \approx U/R_s = I$ [62].

Considering that the steady-state I_2-E characteristics of Fig. 5 change the operation mode to the galvanostatic control, it is possible to observe an important difference in the system's response, i.e., the electrode potential E, upon varying imposed current. Upon cyclic variation of this current a sudden horizontal potential jump occurs which omits the region of the negative resistance, with hysteresis indicating bistability (see Fig. 6).

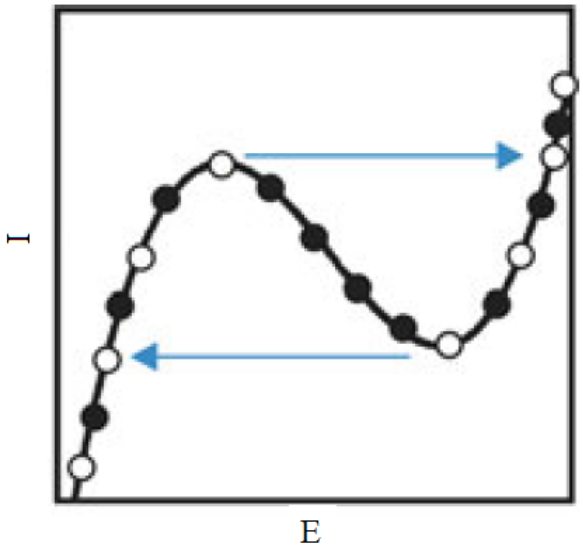

Fig. 6 The dependence of the stability of the steady-states belonging to the negative differential resistance (NDR) region of the N-shape I-E characteristics, on the operation mode: in the potentiostatic mode (filled circle) for negligible (vanishing) serial resistance R_s, and in the galvanostatic mode (open circle) (taken from ref. [62]).

This means that the states belonging to the N-NDR region, which were stable under truly potentiostatic conditions, are unstable under galvanostatic conditions. In other words, only potentiostatic control, in the absence of ohmic drops, allows tracking the entire *I-E* dependence, while in the galvanostatic mode these states are unstable and thus directly inaccessible. For $R_s=0$ the N-NDR system is thus monostable under potentiostatic conditions and bistable under galvanostatic conditions [62].

4. ELECTROCHEMICAL IMPEDANCE SPECTROSCOPY FOR ANALYSIS OF ELECTROCHEMICAL INSTABILITIES

Electrochemical Impedance Spectroscopy (EIS) experiments are highly popular in electrochemical studies, due to the experimental ability to make high-precision measurements. By measuring an electrochemical systems's response to a sinusoidally alternating input signal of small amplitude, and comparing this response or output signal to that derived from a mathematical model of the systems, information can be extracted about the electrode kinetics and its various complications[48].

As the electrical nature of the cell plays such a prime role in its stability features, it is good to know an outline of how the stability problem is approached in electrical engineering. Various authors have already applied these techniques (EIS) to electrochemistry, but due to the recent interest in bifurcations and oscillations in electrochemistry, it seems worthwhile to readdress the so-called frequency domain stability in some detail, not only because of its interesting features, but of the beauty and the power of the method in generalizing and categorizing electrochemical instabilities. It has been shown that a frequency response measurement (i.e. its complex electrical impedance) of the electrochemical system constitutes an elegant way of evaluating its stability and bifurcations [48], and allows also a classification of electrochemical oscillators into well defined types. In fact, due to the linearization involved in the concept of impedance, this stability analysis of the electric (electrochemical) circuits is a specific variant of linear stability analysis [48, 60, 62].

From a theoretical point of view, stability can be defined as the ability of a system to suppress small fluctuations away from the stationary state. If one disposes of a kinetic

model of the system, the stability is assessed by linearizing the kinetic (differential) equations about the stationary state, and subsequently evaluating the local time evolution of small perturbations by solving the linearized differential equations. Stability is uniquely determined by the sign of the eigenvalues of the associated (Jacobian) matrix of coefficients: negative eigenvalues implying a damping out of fluctuations, i.e. stability, and one or more positive eigenvalues implying an exponential growth of fluctuations, i.e. instability [60, 62].

Is it possible to make predictions about the stability of an electrochemical cell without the need for a detailed mathematical model of the system's time evolution? As in electrical engineering, the method for doing this is frequency response analysis [60, 62]. If one determines experimentally a system's frequency spectrum over a broad enough frequency range, one has essentially all the linear information of the system, with which it should be possible to make statements about the stability of the system. Since in the majority of cases, electrochemical cells are stable under truly potentiostatic conditions, and become unstable due to ohmic losses in the external circuit (i.e. a high ohmic drop due to a high electrolyte resistance or a large electrode surface area), and since the influence of the ohmic loss is nothing more than a simple horizontal shift in the complex impedance plane, it is possible to test graphically for the possibility of bifurcations from the impedance characteristics measured potentiostatically.

An electrochemical cell is usually designed in such way that only the working electrode has a significant impedance. The current through the working electrode/electrolyte interface is assumed to be divided between two pathways: a capacitive branch represented by the differential double-layer capacity C_d, and a faradaic branch representing the faradaic (electrochemical) reactions, designated by the unspecific impedance Z_F. The current must pass through an ohmic series resistance R_s, which includes the uncompensated cell resistance and possibly a series resistor deliberately connected in series to the working electrode [48]. In Fig. 7 a general equivalent circuit of an electrochemical cell is shown.

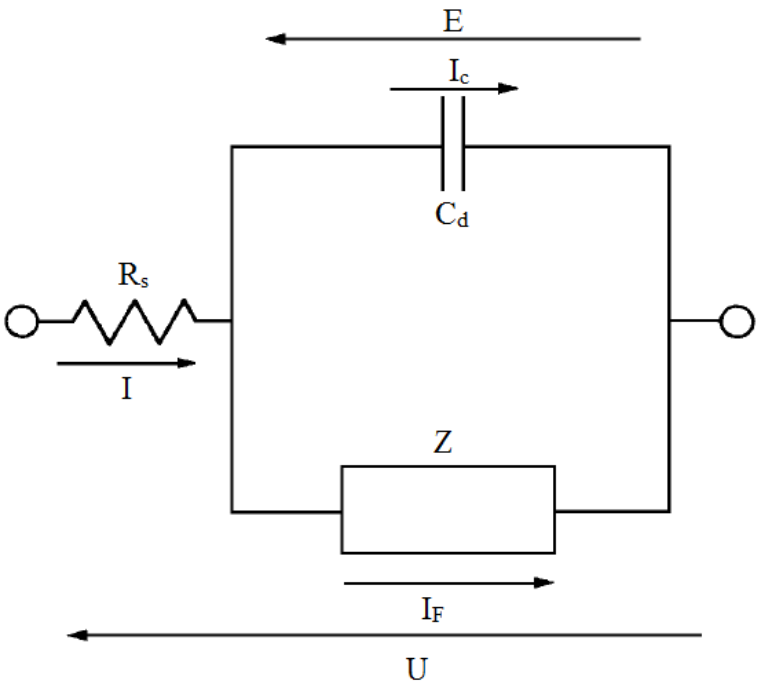

Fig. 7 General equivalent circuit of an electrochemical cell.

Strictly speaking, there is a close coupling between the faradaic current I_F and the charging current I_C of the double layer. Full calculation of the impedance with no separation of the electrode impedance into faradaic and double layer components has been attempted, but the analytical expression of the impedance is particularly complicated. Hence, in most models, it is assumed that the two components can be separated [78]. Then the overall current I is:

$$I = I_F + I_C \tag{8}$$

The behaviour of a nonlinear system can be defined entirely in linear terms if the equivalent linear equations are known at every point of the steady-state characteristics. From an experimental point of view, it is sufficient to measure the impedance of an electrochemical cell about a given polarization point (U_s, I_s), by using a perturbation signal of a very low amplitude. In an *ac* impedance experiment the electrochemical cell is subjected to a small-amplitude sinusoidal perturbation ΔU, superimposed on some applied *dc* bias potential U_s [78]:

$$U = U_s + \Delta U = U_s + \Delta U^{\circ} exp(i\omega t) \tag{9}$$

As a consequence, the electrode potential E will oscillate with the same frequency and the total current I and total current density j usually oscillate with some (frequency-dependent) phase angle φ:

$$E = E_S + \Delta E = E_S + \Delta E° exp(i\omega t) \quad (10)$$

$$I = I_S + \Delta I = I_S + \Delta I° exp[i(\omega t + \varphi)] \quad (11)$$

With $i=\sqrt{-1}$. The cell impedance Z_{cell} is defined as the ratio $\Delta U/\Delta I$, the interfacial impedance Z_{int} as $\Delta E/\Delta I$, and clearly the two are related by $Z_{int}=Z_{cell} - R_s$. Since any impedance is defined by an amplitude ratio and a phase angle, it is convenient to treat them as complex numbers

$$Z = Z' + iZ'' \quad (12)$$

Where $Z'=(\Delta E°/\Delta I°)cos(\varphi)$ and $Z''=(\Delta E°/\Delta I°)sen(\varphi)$. Both R_s and C_d have simple and well-known impedances under sinusoidal excitation, but the faradaic impedance $Z_F(\omega)$ is generally not simple and depends on the detailed kinetics of the electron transfer and the reactant's mass transfer [48].

In the last term (Eq. (12)), one can separate the total impedance Z into the "real" part Z' and the imaginary part Z'', with $\varphi=arctan(Z''/Z')$. Of course, the term "imaginary" refers only to the mathematical notation of the complex number, because both components of impedance are measurable [62]. The impedance spectrum is often constructed in a coordinate system Z' *vs* Z'', called a complex plane (known also as Nyquist, or complex plane plot). In classical electrochemistry, where the imaginary impedance is often related to the capacitive contribution and therefore attains negative values ($Z''= -1/\omega C$), it is plotted on the imaginary axis as positive $-Z''$ values. Then, if Z' is only positive (i.e., the system does not exhibit the negative differential resistance), the typical Nyquist diagram is located in the first quadrant of the Z' vs. $(-Z'')$ complex plane. Thus, it is clear that the systems of interest, with NDR, will exhibit qualitatively different spectra, which will penetrate also other quadrants of the Z' *vs.* $(-Z'')$ complex plane [62, 78].

$Z_F(\omega)$-based models have been derived for a few simple, but representative cases. The simplest model conceivable is that of a resistor, usually referred to as the charge-transfer resistance R_{ct}. This model holds if there is no complication whatsoever to the electron-

transfer process. That is, mass transport is sufficiently fast, the electroactive species do not adsorb and do not chemically react.

$$ox + ne^-_M \longrightarrow red \qquad (13)$$

Where the subscript M indicates metal. The quantity R_{ct} is then defined as $R_{ct}^{-1}=\partial I_F/\partial E$. A common way of representing the results of an *ac* impedance measurement is to plot *Z' vs. (-Z'')* (Fig. 8).

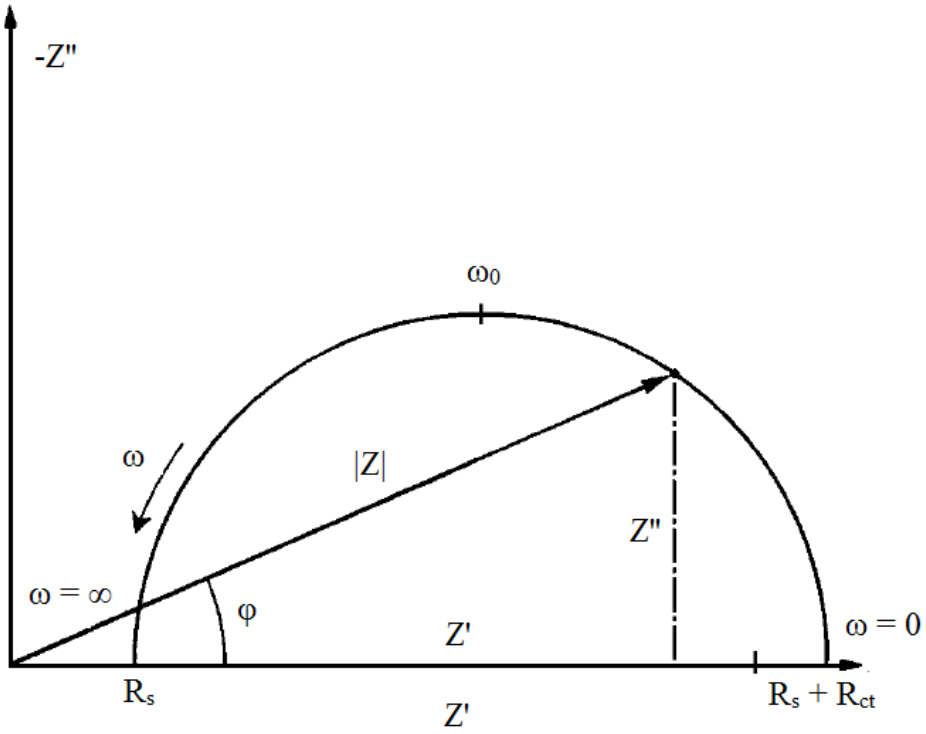

Fig. 8 Complex-plane impedance diagram of Fig. 7 for the case that $Z_F = R_{ct}$.

A usual complication arising in a simple electrochemical reaction is that of a finite mass-transfer rate, that is, when the electrode process is fast or the concentration of the electroactive species is finite, the limitations from the mass-transport rate also manifest themselves in the impedance. The presence of the mass-transport impedance Z_{mt} (called the Warburg impedance Z_W in the case of diffusion) comes from the variation of the concentration profiles in the diffusion layer adjacent to the electrode. For these cases, expressions for the *ac* response of the electrochemical system have to be derived, by including the mass-transport laws pertaining to the system under study [48, 62, 78].

The presence of bifurcations (instabilities) in the dynamics of electrochemical systems is a source of specific problems in the impedance studies. Koper [60] has formulated the general difficulties concerning such measurements. The impedance studies should be performed for the stable steady-state characteristics of an electrochemical system. Let us assume that at the bifurcation point the steady-state, so far stable, loses its stability and the system switches to another attractor (concurrent steady-state or limit cycle). Thus, the impedance measurement on this side of the bifurcation point is not possible. Moreover, the situation is not much better just before this bifurcation [62].

Diagnosis of bifurcation corresponds to theoretical linear stability analysis. As the impedance is based on the linearization of the *I vs. E ac* response around the steady-state, the EIS technique can be used for the analysis of bifurcation in electrochemical systems.

The general principle of application of EIS to the stability analysis of electrochemical systems refers to the phenomenon of resonance between the dynamic characteristics of the electric circuit and the characteristics of the sinusoidal *ac*, small-amplitude perturbation. When the resonance is reached, the impedance of the electric circuit against the externally applied perturbation drops to zero and the perturbing signal is amplified without any phase shift. In particular, if the *ac* perturbing voltage has a non-zero frequency ω_H, equals to the frequency of the circuit at the Hopf bifurcation, then the total impedance should be equal to zero. In turn, if the condition of resonance is reached at zero frequency: ω=0 (of course, in experimental practice is when $\omega \rightarrow 0$), the saddle-node bifurcation is diagnosed from impedance data. The case of ω=0 is identical with the *dc* condition of the electrochemical experiment, so the saddle-node bifurcation requires the NDR, explicitly visible on the steady-state *dc* current-potential dependence, and said NDR is also required for the oscillations [62].

Therefore, the conditions for the bifurcation to occur in potentiostatic (*U* constant) experiments are [48, 62]:

1) A hopf bifurcation*:* $Z(\omega)=0$ for $\omega = \omega_H \neq 0$, and

2) A saddle-node bifurcation: $Z(\omega)=0$ for $\omega = 0$.

These criteria mean that the Nyquist diagram should cross the origin ($Z'=0$, $Z''=0$) of the complex plane for both conditions for *ac* frequency. Fig. 9 illustrates schematically these cases for increasing serial resistances R_s. Note that situations (b) and (c) are rather

theoretical, since from practical point of view the occurrence of the respective bifurcations would mean destabilization of the steady-state, and then the measurements of impedance would be impossible [62].

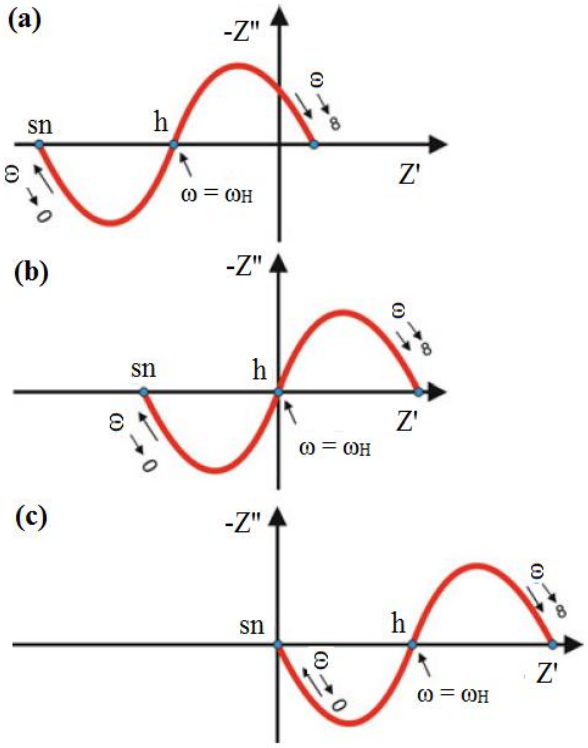

Fig 9 Illustration of the role of increasing serial resistance R_s on the impedance spectra of the NDR system: (a) spectrum for low R_s, insufficient for both Hopf (h) and saddle-node (sn) bifurcations; (b) spectrum for R_s high enough to cause a Hopf bifurcation; (c) spectrum for even higher R_s corresponding to the saddle-node bifurcation (taken from ref. [62]).

The same idea can be applied also to the galvanostatic mode of an electrochemical experiment, when the potential E can exhibit oscillations or bistability [48, 62]. At this moment it is again useful to realize that the galvanostat can be considered a potentiostat, to the output of which a very large (infinite) resistance R_s, in series with the electrochemical cell, was connected and very large (infinite) voltage U was applied, with the ratio $U/R_s = I$ defining the imposed current. Since this serial resistance is so large, any change of the electrochemical cell's resistance (impedance), caused by the course of an electrochemical process, is relatively so low that $R_s + R_e(Z_F) \approx R_s$ and the imposed current remains almost constant. This also means that in the galvanostatic mode, contrary to the potentiostatic one, it is not possible to adjust R_s from zero to any desirable value, since R_s is already present and is always very high. As a consequence, the condition of resonance requires

compensation of very high positive resistance with equally high real negative impedance of the electrochemical cell: $Z' \rightarrow 0$, which means equivalently zero real faradaic admittance $Y'=0$.

Therefore, the conditions for the respective bifurcations for the galvanostatic experiment are [48, 62]:

1) A hopf bifurcation: $Y(\omega)=0$ for $\omega = \omega_H \neq 0$,

2) A saddle-node bifurcation: $Y(\omega)=0$ for $\omega = 0$.

Although under galvanostatic conditions the insertion of an additional serial resistance is not necessary for these bifurcations to occur, the presence of such resistance would be required again under potentiostatic conditions, when the ohmic drops have to be coupled with the NDR. Thus, it is concluded that electrochemical systems exhibiting potential oscillations under galvanostatic conditions, should also exhibit current oscillations under potentiostatic conditions, provided that in the latter case an appropriate serial resistance is present in the circuit.

It is instructive to compare typical impedance spectra of the systems that can exhibit oscillations under potentiostatic conditions to the ones under galvanostatic conditions. Figure (10) illustrates typical Nyquist spectra for the processes that will exhibit oscillations and bistability under potentiostatic and galvanostatic conditions.

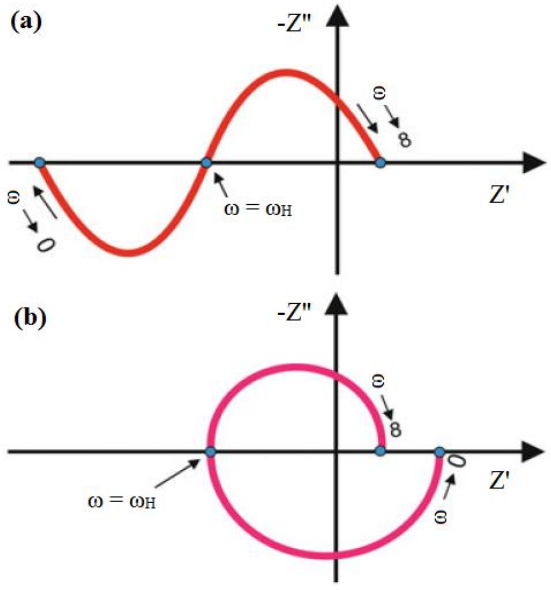

Fig. 10 Schematic shape of the Nyquist diagrams for the systems with (a) explicit (observable at ω=0) NDR region and (b) hidden NDR region (observable only at intermediate $0<\omega<\infty$ frequencies) typical of HNDR systems (taken from ref. [62]).

Let us analyze these two spectra, first from Fig. 10 (a). If we increase the serial resistance R_s from low value (as showing in the picture) to the appropriately large values, then the entire spectrum shifts to the right, and when R_s compensates the negative real impedance Z' and $Z''\rightarrow 0$ at $\omega=\omega_H$, the total impedance of the circuit becomes zero for the first time during the increase in R_s. Then the Hopf bifurcation, i.e., the onset of oscillations, takes place. Upon further increase of R_s the system still exhibits oscillations, until the compensation of the negative real impedance for $\omega=0$ takes place again. At this point, the system undergoes the saddle-node bifurcation and the appearing stable node takes control over the system's dynamics, i.e., the oscillations cease to exist. Upon further increase in R_s no other bifurcation occurs, so the system does not return to the oscillatory regime, guarantying that the galvanostatic oscillations are not possible.

Now consider the galvanostatic regime, remembering that it means measurement involving the potentiostat with very large serial resistance present. In terms of Fig. 10 (a) such a high (theoretically infinite) resistance means that we are always far beyond the second, saddle-node bifurcation, when no oscillations exist. Therefore the system characterized with spectrum in Fig. 10 (a), with explicit NDR in the *dc* current-potential characteristics, can exhibit only bistability under galvanostatic conditions [62].

It becomes obvious that the system in which the electrode potential oscillates under galvanostatic conditions must be characterized with qualitatively different impedance spectrum, excluding the above sequence of the Hopf bifurcation, followed by any saddle-node bifurcation upon increasing R_s. In order to avoid such saddle-node bifurcation, for low (tending to zero) *ac* frequencies the spectrum must return to positive real impedance, as in Figure 10 (b).

Since $\omega=0$ means *de facto dc* conditions, the corresponding limiting positive real resistance is equivalent to the positive slope of the steady-state *dc* current-potential characteristics. It also means that although the negative resistance is present in the system's characteristics, it does not manifest itself explicitly on *dc* current-potential dependence, at the potential E for which the spectrum in Fig. 10 (b) was collected. This negative impedance can only be revealed in impedance measurements for the non-zero, intermediate values of ω and therefore remains "hidden" under *dc* conditions. Oscillatory systems of this type belong to the so-called hidden NDR or HNDR type, the idea of which was introduced

by Koper and Sluyters [55]. Obviously, the negative impedance can remain hidden if at least two processes overlap: one, relatively fast, with the NDR characteristics and the other one relatively slow, with the positive slope. The slow process manifests itself in the spectrum only at low frequencies, while the faster process characterized with the negative impedance reveals itself at the intermediate frequencies.

5. CLASSIFICATION OF ELECTROCHEMICAL OSCILLATORS

Spontaneous kinetic oscillations of the electrical current or potential are frequently occurring temporal behaviours of electrochemical processes, when nonlinear chemical kinetics combines with external electrical circuit constraints [10-71]. Some authors have classified the individual electrochemical oscillators with respect to various criteria: the chemistry involved [11], the overall direction of the electron transfer at the working electrode [11] or the operating conditions [60].

The first important mechanistic classification [79] involved the distinction between chemical and electrochemical oscillatory systems. In the former systems a purely chemical autocatalysis, merely accompanied by chemical charge-transfer steps at the electrode, causes the dynamical instability. While in the latter systems, it is the interplay of chemical and electrical variables which apparently originates the instability.

A stability study and categorization of electrochemical oscillators by impedance spectroscopy was proposed in 1996 by Koper [60]. Just like mathematical linear stability analysis allows us to find the qualitative type of the phase trajectories of the systems of linear(ized) differential equations without obtaining their explicit solutions, the impedance spectroscopy, being the electrochemical variant of linear stability analysis, allows one to categorize electrochemical oscillators without studying the detailed mechanism of the given process, by looking only at the shape of the impedance spectrum [60-62]. The ability of impedance spectroscopy to make predictions about the occurrence of oscillations leads in a natural way to a classification of electrochemical oscillators into two categories, depending on the kinetic nature of the negative faradaic impedance [60]. In other words, based on characteristic features of a systems's impedance spectrum, the possible conditions for bifurcation occurrence can be predicted [61].

Koper divided electrochemical oscillator into three classes [60]: Class 1-Oscillations (of current) occur under truly potentiostatic conditions, Class 2-Oscillations only under potentiostatic conditions with sufficiently large ohmic drop, Class 3-Oscillations under galvanostatic conditions and under potentiostatic conditions with sufficiently large ohmic drop. Strassser *et al*. [61] distinguished four main oscillator categories, depending on the mechanistic role of the potential drop across the electrode/electrolyte interface (double layer potential) and of the chemical species involved, including one class more, extending the classification presented by Koper.

Class I: strictly potentiostatic oscillators

In this class of oscillators the electrode potential *E* is a non-essential dynamic variable; it essentially represents purely chemical oscillators involving at least one electrochemical step, that is, one of the chemical reactions is associated with charge-transfer at an electrode interface; this allows us to observe the chemical oscillations by means of the electrochemical element. The existence of the NDR region is thus not necessary for the oscillations, and neither is a non-zero serial resistance. However, if such resistance is present, the oscillating current causes, through the ohmic drops, an oscillatory variation of the electrode potential and then the electrochemical process can affect the concentration of the involved species, interacting in this way with the chemical oscillatory process.

Classs II: Oscillators with the S-shaped NDR

Class II is directly related to Class I; yet their mechanistic features are clearly distinct from strictly potentiostatic oscillators. Similarly to Class I, concentrations of chemical species are the dynamic variables involved, but now the electrode potential appears to be an essential system variable. The electrode potential supplies a slow, negative feedback. This is why under strictly potentiostatic conditions all oscillatory behaviour ceases, and the destabilizing chemical feature becomes visible in the stationary current-potential curve, which manifests itself in a bistable profile. Depending on the relation between autocatalytic species and faradaic current, the bistable adsorption profile ideally gives rise to a S- or Z-shape current-potential profile. Since the stationary polarisation curve must cross the zero-

current axis at some point, an ideal Z-shape voltammogram cannot exist in a real electrochemical system, and it usually becomes a complex N-shape curve. The latter profile, however, is unable to yield sustained current or potential oscillations when the potential is the slow feedback variable. Therefore only S-shape voltammetric curves need to be considered.

Class III: N-NDR oscillators

The majority of known electrochemical oscillators fall into this class. Examples of this class of oscillator are given by Krischer [80]. Class III involves the electrical double layer potential as an autocatalytic variable leading to a negative differential resistance (NDR), and the systems of this category are usually referred to as "NDR-oscillators', due to the indispensable presence of the negative differential resistance [48, 60-63, 80]. The electrode potential E is an essential variable, more strictly, an autocatalytic (positive feedback) variable. Purely chemical instabilities can be completely absent. It is also important that the current oscillations occur exclusively on the stationary current-potential branch of negative slope. At vanishing ohmic resistance, the potential region of negative slope naturally yields a monostable N-shape voltammetric profile (Fig. 11 (a)). The underlying chemical cause for the negative regulation can be very diverse, such as Frumkin double layer effects, adsorption and desorption of a catalyst, or competitive adsorption. The electrochemical system with such characteristics, for a given externally applied voltage U, exhibits current oscillations in the presence of appropriate ohmic potential drops, caused by the serial resistance R_s, but under galvanostatic conditions only bistability is observed, since then the NDR region is a collection of unstable (saddle-type), and thus directly inaccessible, steady-states [62].

From the theoretical considerations one can formulate the necessary and sufficient mechanistic ingredients of a NDR oscillator as follows [61]:

- The principal charge-transfer process consists of one or more dependent faradaic current carriers with at least one exhibiting an N-shape current-potential profile, and
- A slow chemical species, consumed by all current carriers, which is formed or transported by a potential-independent process.

Figure 11 (a-c) illustrates schematically the cyclic voltammetric behaviour of NDR oscillators at different conditions, and its characteristic impedance spectrum is given in Fig. 11 (d).

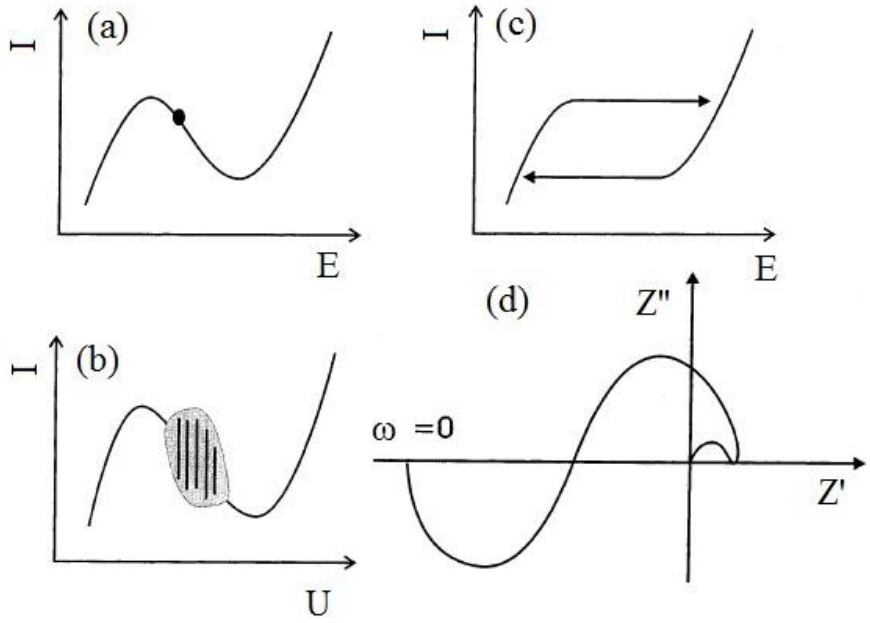

Fig. 11 Current-potential characteristics as well as characteristic impedance behaviour for Class III (NDR) oscillators: (a) potentiostatic *I*/*E* behaviour under strictly potentiostatic conditions; the black solid circle denotes the point associated with the impedance spectrum given in (d); (b) potentiostatic *I*/*U* behaviour for finite values of the ohmic resistance; (c) galvanostatic *I*/E behaviour; (d) impedance spectrum for a Class III NDR oscillator at the current-potential marked with a black circle in (a) (taken from ref. [61]).

Class IV: HNDR oscillators

This class shares some similar characteristics with Class III. Insofar as the double layer potential is the autocatalytic system variable due to a negative differential resistance, with the chemical species typically providing the slow dynamical feedback. Similarly, potentiostatic current oscillations only occur at finite ohmic resistances. However, systems of Class IV also exhibit oscillations under galvanostatic conditions (without ohmic drop). These systems show a potentiostatic Hopf bifurcation, associated with sustained current oscillations on a polarization branch with positive regulation (positive zero-frequency impedance), as well as galvanostatic potential oscillations. Consequently, at these points, a negative differential resistance must be operative on a fast time-scale, that is, must be hidden on the stationary polarization curve. In the literature, these electrochemical oscillators are referred as HNDR oscillators. These systems are characterized by a hidden

negative impedance, which manifests itself as the negative impedance for a range of non-zero *ac* frequencies, with a positive zero frequency impedance (corresponding to the positive slope of the *dc* current-potential curve).

Figure 12 (a-c) illustrates schematically the cyclic voltammetric behaviour of HNDR oscillators at different conditions, and its characteristic impedance spectrum is given in Fig. 12 (d)

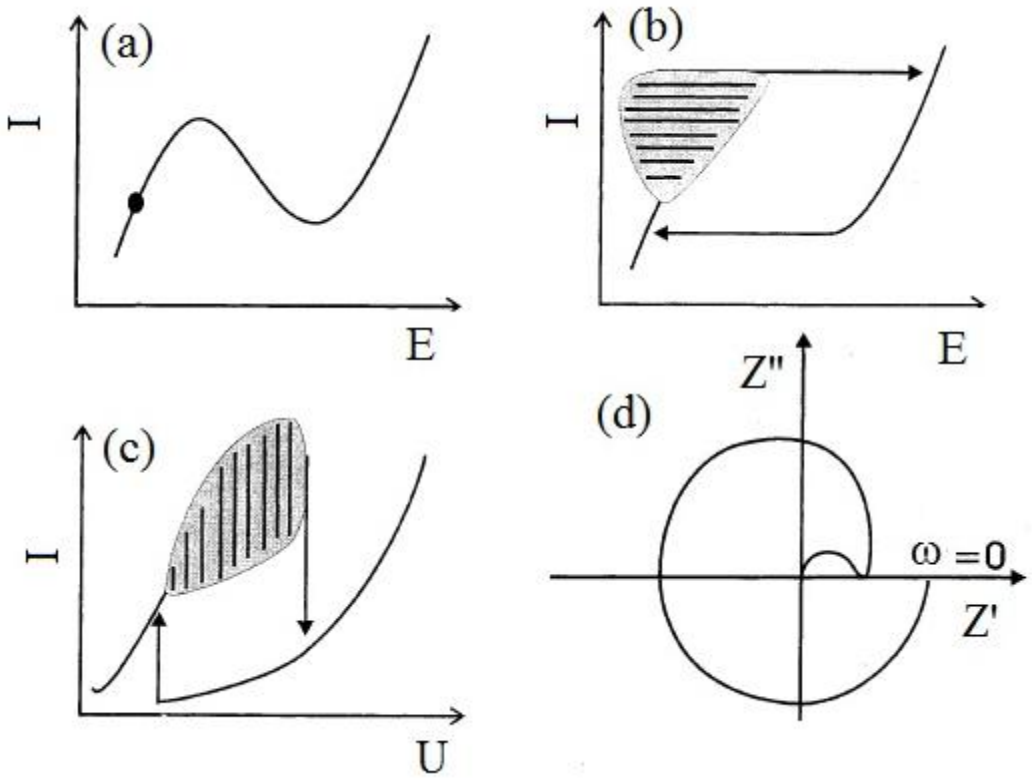

Fig. 12 Current-potential characteristics as well as characteristic impedance behaviour for Class IV (H-NDR) oscillators: (a) potentiostatic *I*/*E* behaviour under strictly potentiostatic conditions; the black solid circle denotes the point associated with the impedance spectrum given in (d); (b) galvanostatic *I*/E behaviour; (c) potentiostatic *I*/*U* behaviour for finite values of the ohmic resistances; (d) impedance spectrum for a Class IV HNDR oscillator at the current-potential marked with a black circle in (a) (taken from ref. [61]).

For such impedance characteristics, two coupled potential-dependent processes have to be present: a relatively fast process giving rise to a negative impedance and a slower process of a positive impedance, which dominates the steady-state *dc* current-potential characteristics. The presence of an appropiate external resistance is not necessary for the

galvanostatic oscillations, but is required for the onset of potentiostatic (constant *U*) oscillations of the current. [62].

It appeared to be convenient to subdivide the HNDR category into at least three subcategories, since all experimental features mentioned so far are generally valid for any HNDR oscillator. Each subcategory exhibits specific mechanistic and experimental features on which the subdivision is based. Strasser suggested dividing Class IV oscillators into the following subcategories [61]:

Class IV.1. Potential-dependent source of the inhibitor

The simplest way to obtain an HNDR oscillator from a NDR model is to assume a potential-dependent source term for the slow, inhibiting species.

Class IV.2. The H_2/formic acid group

This category involves an independent current carrier, that is, a faradaic process consuming non-essential species only; by itself it exhibits a normal potential regulation. The model calculations show that the current carrier may even be potential-independent (diffusion limited current). At the model level, description of dynamical system of this type requires three variables: electrode potential *E*, an essential fast chemical species and an essential slow chemical species, producing the negative feedback. The dynamics of the slow species may completely cover up the N-shape potential profile of the fast subsystem.

Class IV.3. The IO^-_3 group

This subcategory is born from a typical NDR system by adding and appropriate independent current carrier with the usual Butler-Volmer kinetic characteristics. In this case the independent current carrier does not consume the slow chemical variable. Instead, this additional current-providing reaction may proceed on free (not blocked) surface sites. This additional current overlaps with the NDR region, hiding it under *dc* conditions and in this way transforming the NDR into an HNDR oscillator.

Based on the above classification, Strasser *et al.* [61] have suggested a systematic experimental strategy for the classification of the electrochemical oscillators (Fig. 13):

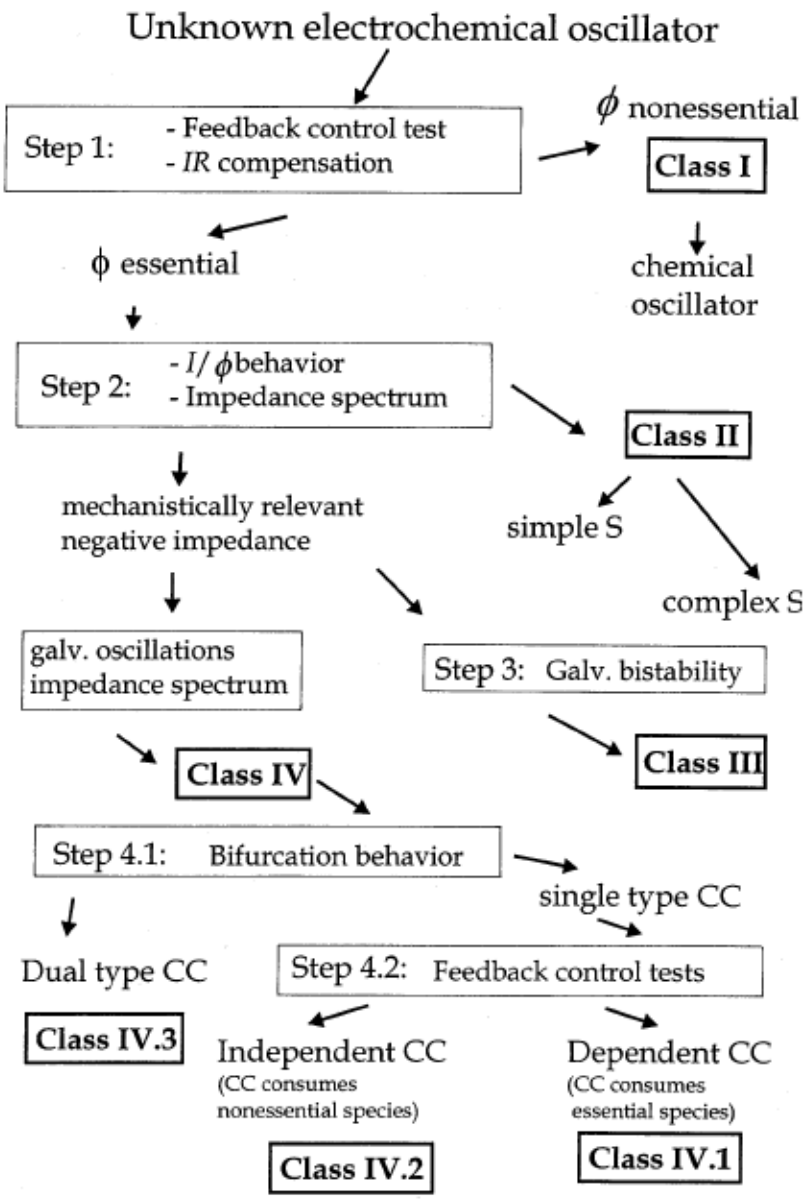

Fig. 13 Summary of an operational method for the experimental classification of an unknown electrochemical oscillator (CC=current carrier) (taken from ref. [61]).

Even if these principal four classes represent a complete classification scheme, it is not excluded that the introduction of further subcategories may become necessary in the future, because of new discovered electrochemical oscillators with different oscillatory mechanisms [62, 63]. As the above classification does not cover the spatiotemporal and spatial pattern formation, as well as it omits instabilities caused by electrochemically generated convection, several modifications or extensions have been proposed [29, 62].

6. NONLINEAR DYNAMICS

Dynamics is the subject that deals with change, with systems that evolve in time. Whether the system in question settles down to equilibrium, keeps repeating in cycles, or does something more complicated, it is dynamics that is used to analyze the behaviour.

The system's behaviour can be linear or nonlinear. To understand the distinction between linearity and nonlinearity, recall that a mathematical equation can be thought of as a function (something that maps inputs to outputs). The equation $y = x$, for instance, is equivalent to a function that takes as its input a value for x and produces as its output a value for y. The same is true of $y = x^2$.

The equation $y = x$ is linear because adding together inputs yields the sum of their respective outputs: 1 = 1, 2 = 2, and 1 + 2 = 1 + 2. But that is not true of $y = x^2$: if x is 1, y is 1; if x is 2, y is 4; but if x is 3, y is not 5.

This example illustrates the origin of the term "linear": the graph of $y = x$ is a straight line, while the graph of $y = x^2$ is a curve. But the basic definition of linearity holds for much more complicated equations, such as the differential equations used in engineering to describe dynamic systems. Nonlinear systems are characterized by no complying with the principle of superposition.

Nonlinear equations are difficult to solve, and are commonly approximated by linear equations (linearization). This works well up to some accuracy and some range for the input values, but some interesting phenomena such as chaos are hidden by linearization. It follows that some aspects of the behaviour of a nonlinear system appear commonly to be chaotic or unpredictable. Although such chaotic behavior may resemble random behaviour, it is absolutely not random.

It is important to distinguish between the terms "deterministic" and "stochastic" chaos. Deterministic chaos differs from stochastic aperiodicity in that it has a deeply buried order under its apparent disorder [81]. Deterministic chaos is somewhat puzzling to the extent that, despite being a phenomenon governed by simple deterministic laws, there is no way no predict its behavior. The mathematical models associated to a phenomenon of deterministic chaos cannot be solved by analytical procedures.

One of the defining characteristics of deterministic chaotic behaviour is the sensivity to initial conditions. Two trajectories that start from initial points as close as possible end up, losing all correlation between them, after some short time.

Nowadays, there are many tools for analyzing the system's nonlinear behaviour from the time series (the monitoring of the system's variables in time), without knowing the laws governing the phenomenon.

A phase space of a dynamical system is a multidimensional space where the coordinates are the pertinent variables of the system [81]. All the possible states of the system are represented, with each possible state corresponding to one unique point in the space phase. A phase portrait is a representation of the trajectories of a dynamical system in the phase plane. Similar to a direction field, a phase portrait is a graphical tool to visualize how the solutions of a given system of differential equations would behave in the long run. In this context, the Cartesian plane where the phase portrait resides is called the phase plane. The parametric curves traced by the solutions are the trajectories. A coordinate plane with axes being the values of the two state variables, say (q, p), it is a two-dimensional case of the general n-dimensional phase space.

For nonlinear systems, there is typically no hope of finding the trajectories (solutions) analytically. Even when explicit formulas are available, they are often too complicated to provide much insight. Instead, the objective is to determine the qualitative behaviour of the solutions. The goal is then to find the system's phase portrait directly [82].

An enormous variety of phase portraits is possible. Some of the salient features of any phase portrait are shown in Fig. 14 [82]:

1) Fixed points, like A, B, and C. These points correspond to steady states or equilibria of the system. Fixed points can be attractors or repellers. The representative point in phase space of a system approaching a steady state converges toward a fixed point, which thus is an "attractor" for these conditions. The word attractor in this context refers to a special trajectory in phase space which other trajectories approach regardless of initial conditions [81].

2) The closed orbits represented by D. It corresponds to periodic solutions. The attractor is a closed curve: the limit cycle, when a system's behaviour is periodic.

3) The arrangement of trajectories near the closed orbit D is different. There are limit cycles that have defined a state of attraction (attractor or repeller).

4) The stability or instability of the fixed points and closed orbits. Here, the fixed points A, B, and C are unstable, because nearby trajectories tend to move away from them, whereas the closed orbit D is stable.

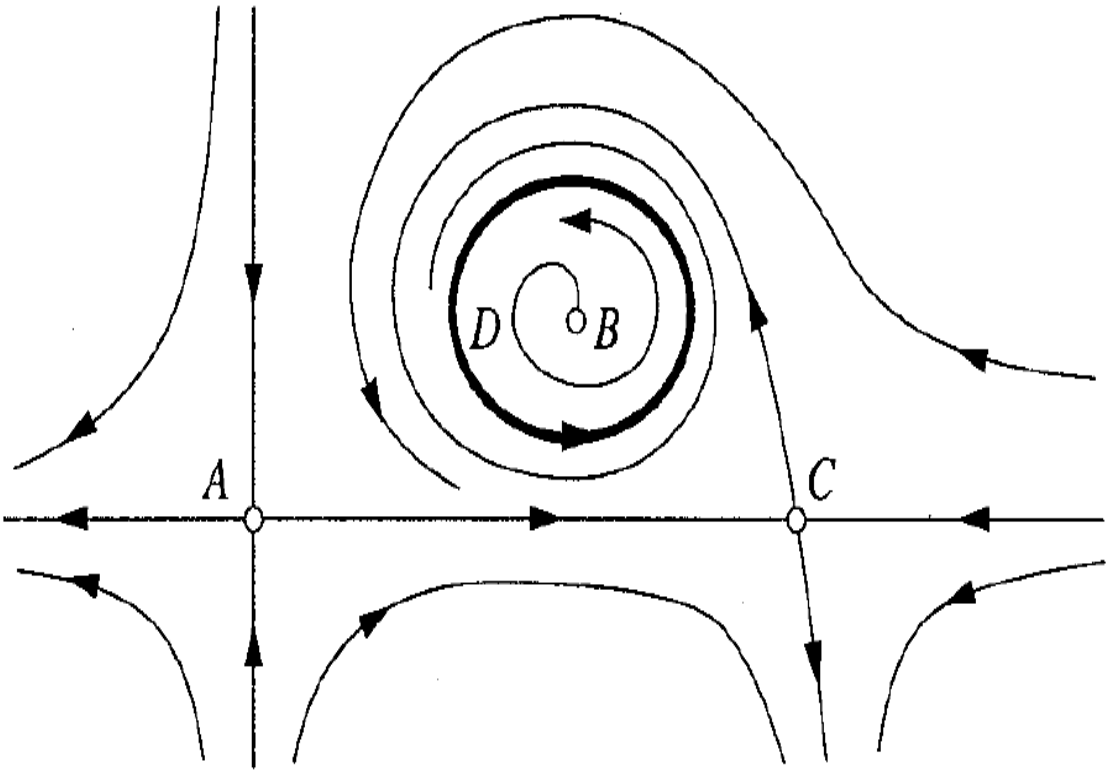

Fig. 14 Representation of the most salient features of any phase portrait (taken from ref. 82).

Quasiperiodic behaviour appears as an open path of infinite period. The name comes from the fact that observed at short times, it appears to be periodic. Periodic behaviour is defined as recurring at regular intervals, such as "every 1 hour", while quasiperiodic behaviour is a pattern of recurrence with a component of unpredictability. Strange attractors exist in regimes exhibiting deterministic chaos. A strange attractor (Fig. 15) looks similar to a closed curve, staying in a roughly circular volume of phase space, but it never closes on itself.

Nonlinear analysis has been a useful tool for the study of instabilities in electrochemical systems [81-86]. A data-analysis technique, known as attractor

reconstruction, permits us to visualise the changes in the dynamical variables. The claim is that for systems governed by an attractor, the dynamics in the full phase space can be reconstructed from measurements of just a single time series. For instance, define a two-dimensional vector $\boldsymbol{x}(t)=(B(t),\ B(t+\tau))$ for some delay $\tau>0$. Then the time series $B(t)$ generates a trajectory $\boldsymbol{x}(t)$ in a two-dimensional phase space (attractor). Once established a phase space for the system, such that specifying a point in this space specifies the state of the system, then the dynamics of the system can be studied by studying the dynamics in the phase space [81-82].

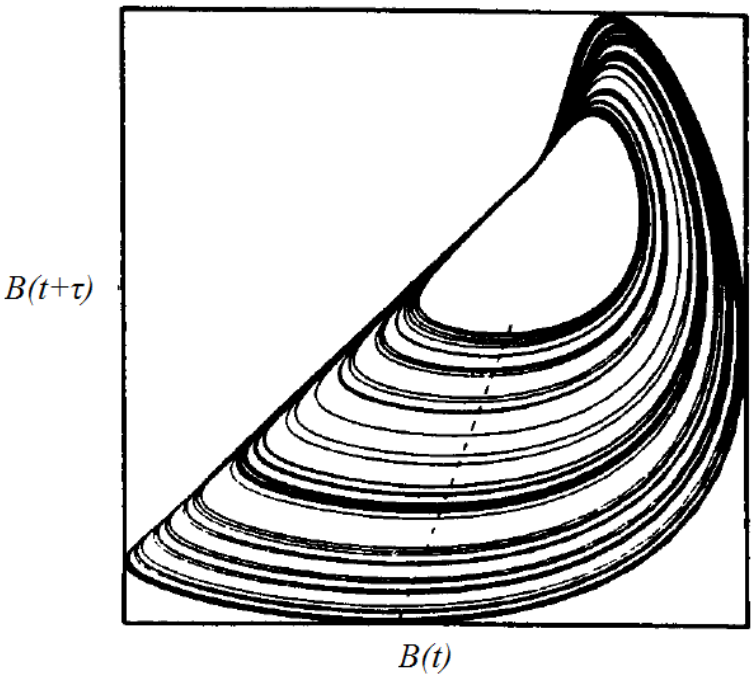

Fig. 15 Two-dimensional projection of the phase space attractor obtained from chaotic data in the BZ reaction by the delay method (taken from ref. 87).

Chapter 3

Cadmium/cyanide electrochemical oscillator

Dynamical behaviour observed during the electrodissolution of metals has received more attention than other types of electrochemical reactions. Few papers in literature report on oscillatory behaviour during the electrodeposition of metals, making this last phenomenon a very interesting field of research. The dynamics during the electrodeposition of cadmium in solutions containing cyanide ions will be discussed in this section. Electrochemical experiments were done to obtain and characterize the dynamical behaviour of the process. Finally, the attractor reconstruction was used to discuss the oscillations observed in the electrochemical experiments.

1. EXPERIMENTAL

Cadmium was deposited from solutions containing different concentration ratios of Cd^{2+} as $CdSO_4 \cdot 8/3\ H_2O$ and CN^- as KCN. The electrolytes were prepared using chemicals of *pro analysis* purity and distilled water. Table I shows the six solutions, with different Cd^{2+}/CN^- concentration ratios, prepared for the electrochemical experiments, increasing the Cd concentration.

Table I. Cd^{2+}/CN^- concentration ratios of the solutions used for electrodeposition of Cd.

Solution	Cd^{2+} concentration, (M)	CN^- concentration, (M)	Cd^{2+}/CN^- concentration ratio
S1	0.039	0.583	0.067
S2	0.074		0.127
S3	0.117		0.201
S4	0.148		0.254
S5	0.156		0.268
S6	0.195		0.334

The electrochemical experiments were performed in a 100 cm^3 three-electrode glass cell at room temperature. Platinum (Goodfellow, 99.95%, temper as rolled, 1 cm^2) was used

as working electrode, and a mesh platinum gauze (Alfa Aesar, 99.95%) as counter electrode. Preliminary preparation of the platinum working electrode includes pickling in a 50% solution of nitric acid, followed by polishing with 0.3 micron micropolish powder and cleaning with distilled water in a Branson ultrasonic cleaner equipment. A saturated calomel electrode ($E_{Hg/Hg2Cl2}$=0.2444 V vs SHE) was used as reference.

The current-potential curves, potentiostatic and galvanostatic time series experiments were carried out by means of a computerized potentiostat/galvanostat Series G 750 (Gamry Instruments Inc., Warminster, Pennsylvania) using the PHE 200 software; the Electrochemical Impedance Spectroscopy (EIS) was assessed with the EIS 300 software. All potentials are referred to a saturate calomel electrode (SCE). The time series of the potentiostatic and galvanostatic curves were recorded with a sampling period of 0.001 s, and because of this, the time registered was limited to 260 s. The selected sampling period was chosen because the shape of the recorded curves depends on the number of obtained data. When the experiments were realized at longer time scales, the systems slowly drifted, which tended to shift the oscillatory region to more anodic potential and current values, probably as a result of the change in working electrode surface. The time series of the oscillations at galvanostatic and potentiostatic conditions were analyzed by the Fast Fourier Transform (FFT) and space phase projections.

The surface morphology of the Cd coatings electrodeposited on Cu electrodes was revealed using the scanning electronic microscopy (SEM) XL30-ESEM (Philips, Holland).

2. RESULTS AND DISCUSSION

2.1. The voltammetric characteristics

The cathodic current–potential curves for Cd electrodeposition from the solution containing a Cd^{2+}/CN^{-}=0.067 concentration ratio (solution S1), on a vertical platinum electrode, under potential and current scanning are shown in Fig. 16.

The polarisation curve obtained by a potential sweep (Fig. 16 (a)) shows that electrodeposition of Cd starts at -1.5 V. A flat area in the polarisation curve is observed at a potential of -1.75 V, which could be assumed as the limiting current density for the Cd

reduction process. Hydrogen evolution was observed, from the surface of the working electrode, at potentials more negative than -1.85 V.

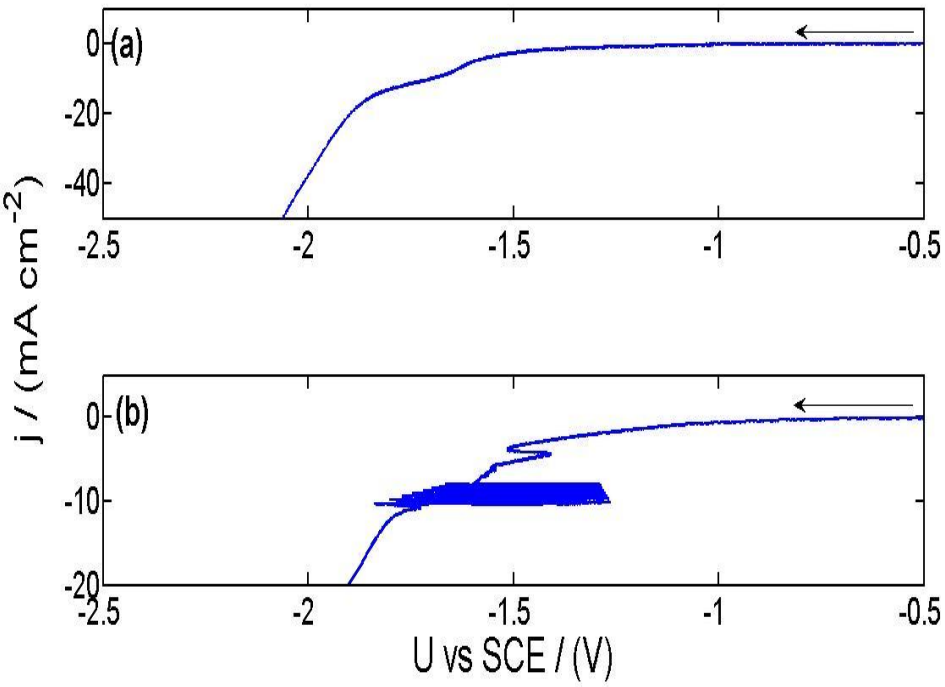

Fig. 16 Cathodic polarisation curves for deposition of Cd at Cd^{2+}/CN^{-}=0.067 concentration ratio, on a Pt electrode: (a) under potential sweep at 10 mV s^{-1}; (b) under current sweep at 0.1 mA cm^{-2} s^{-1}.

Figure 16 (b) presents the cathodic polarisation curve for Cd electrodeposition obtained by current sweeping, when cathodic potential oscillations were registered. The onset of potential oscillations occurs approximately at a current density of -5 mA cm^{-2}. These potential oscillations are accompanied by pulsating hydrogen evolution. When the current density is higher than -11 mA cm^{-2}, the oscillations stop and intensive hydrogen evolution is observed. The oscillations increase their amplitude, because of the higher imposed current. It was not possible to register current oscillations during the potentiodynamic polarisation (Fig. 16 (a)).

In order to compare the behaviour of the electrodeposition of Cd, at Cd^{2+}/CN^{-} concentration ratios higher than 0.067, polarisation curves were obtained potentio- and galvanodynamically. Figure 17 shows the characteristics of the polarisation curves at different Cd^{2+}/CN^{-} concentration ratios (Table I), for the Cd electrodeposition.

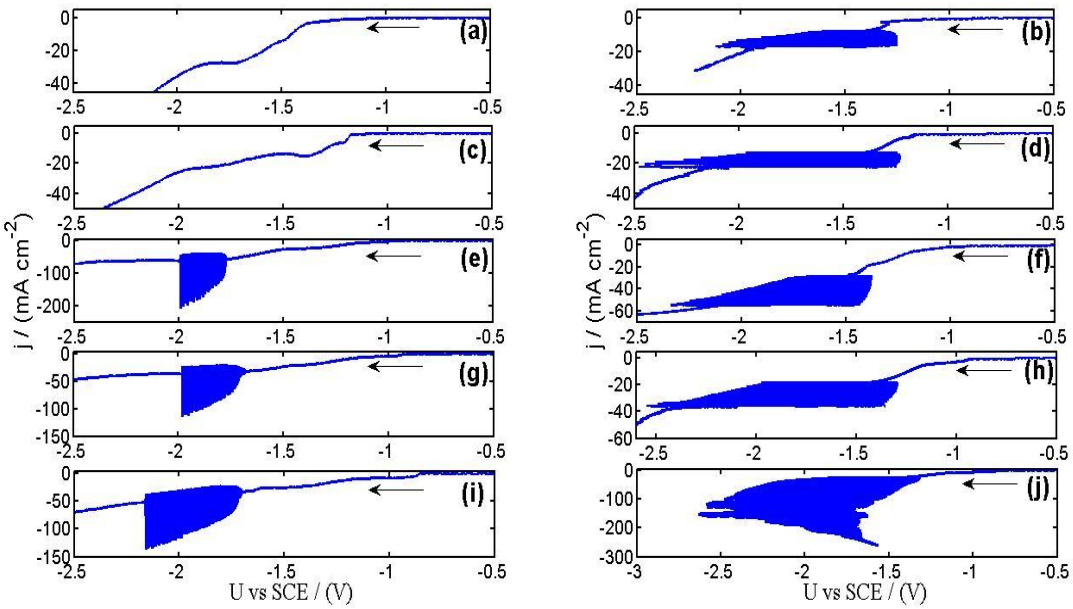

Fig. 17 Cathodic polarisation curves for electrodeposition of Cd on Pt under potential sweep at 10 mV s^{-1} for a Cd^{2+}/CN^- concentration ratio: (a) 0.127, (c) 0.201, (e) 0.254, (g) 0.268, (i) 0.334; under current sweep at 0.1 mA cm^{-2} $s^{-1}$for a Cd^{2+}/CN^- concentration ratio: (b) 0.127, (d) 0.201, (f) 0.254, (h) 0.268, (j) 0.334.

When the concentration of Cd ions in the solution is increased (as larger Cd^{2+}/CN^- concentration ratio is used), the electrodeposition of Cd starts at less negative potentials.

It can be noted that current oscillations appear at Cd^{2+}/CN^- concentration ratio of 0.254 (Fig. 17 (e)), when the potential reaches -1.70 V, accompanied by continuous hydrogen evolution from the surface of the electrode [70, 88]. However, current oscillations disappear at potentials more negative than -1.90 V, where intensive hydrogen evolution can be observed. When the Cd concentration in the solution increases, the current oscillations appear at less negative potentials, and in a wider range (Fig. 17 (g)-(i)). Similarly to the case shown in Fig. 16, the amplitude of the current oscillations increases at higher potentials.

The polarisation curves obtained by current scanning showed that the potential oscillations appear at all the concentration ratios used (Fig. 17 (b), (d), (f), (h), (i)). The onset of potential oscillations occurs at higher current densities when the concentration ratio of the solution is increased. These potential oscillations are accompanied by pulsating hydrogen evolution. The higher the concentration ratio of the solution the higher the applied current density needed to cease the potential oscillations.

2.2. Electrochemical impedance spectroscopy

The electrochemical impedance spectra were recorded for Cd electrodeposition, at different potentials, chosen from the potentiodynamic current-potential curves with Cd^{2+}/CN^- concentration ratios of 0.127 (Fig. 18 (a)) and 0.254 (Fig. 18 (b)). The impedance experiments showed that the electrodeposition of Cd from cyanide electrolytes has even more complex characteristics than it could be supposed only from the *dc* measurements. The impedance spectrum for Cd^{2+}/CN^-=0.127 at -1.20 V (inset (1) in Fig.18 (a)) presents only positive real impedance in the first descending branch (positive slope in the polarisation curve). The impedance experiment at -1.40 V (inset (2) in Fig. 18 (a)) showed that the impedance spectrum enters in the region of negative real impedance in a range of non-zero frequencies. This behaviour, which corresponds to the plateau of the current-potential curve, suggests the presence of a hidden negative resistance under *dc* conditions during Cd electrodeposition, belonging to Class IV (HNDR oscillator), as proposed in the classification given by Strasser *et al.* [61]. The same impedance characteristics were registered for the electrodeposition of Cd from a solution with a higher concentration ratio (0.254), in similar points of the current-potential curve (Fig. 18 (b)).

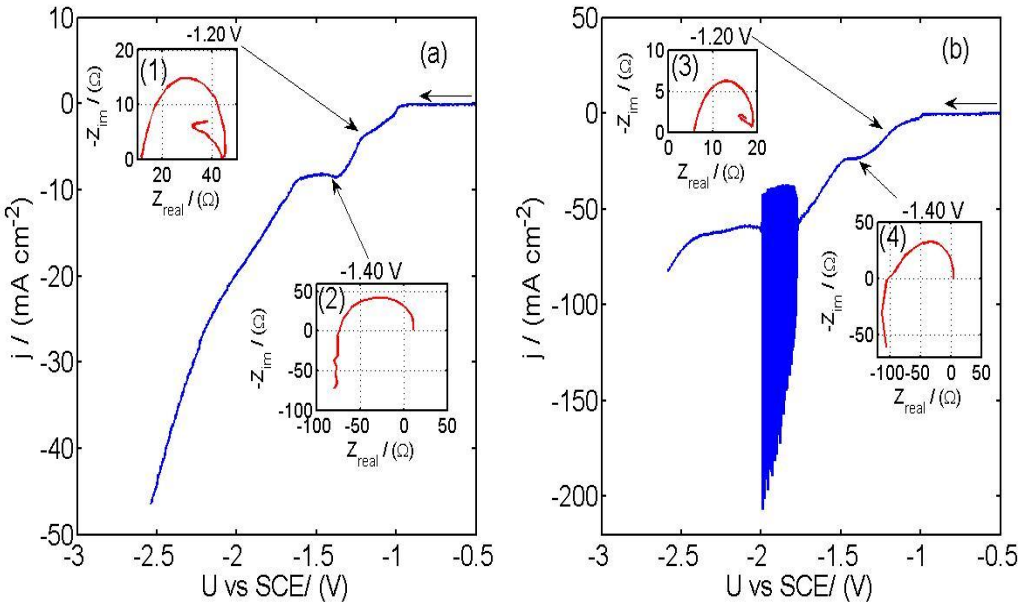

Fig. 18 Potendynamic current-potential curve for the electrodeposition of cadmium at different conditions: (a) Cd^{2+}/CN^-=0.127, (b) Cd^{2+}/CN^-=0.254. Insets (1) and (3) are the impedance spectra at -1.20 V and (2) y (4) at -1.40 V.

Because the attempts to measure the impedance spectra at frequencies lower than those indicated in Figs. 18 ((a)-(b)) were unsuccessful, the electrochemical impedance spectra presented in Fig. 18 ((2)-(3)) do not reveal the whole shape expected for the HNDR oscillator. It is expected that the loop beginning and end must have positive real impedance, for both zero and infinite frequencies, with the negative real impedance manifesting itself only for its intermediate regions. Based on the present results, it can be proposed that the electrodeposition of cadmium from a cyanide electrolyte on a vertical Pt electrode belongs to the HN-NDR type: an oscillator with a negative impedance spectrum in a region of positive slope in the N-Shape current-potential curve, with an oscillatory behaviour observed not only under galvanostatic conditions, but also under potentiostatic conditions, with adequate ohmic drops (Fig. 17).

It was mentioned in the classification of electrochemical oscillators that Class IV (HNDR oscillators) presents potential oscillations under galvanostatic conditions and current oscillations under potentiostatic conditions at high ohmic drops. In Figure 17 it is observed that galvanostatic potential oscillations appear at all the studied Cd^{2+}/CN^- concentration ratios. The current oscillations can be registered for solutions with a Cd^{2+}/CN^-=0.254 concentration ratio and higher (Figs. 17 (e), (g) and (i)), but not for those solutions with the lower concentration ratios (Figs. 17 (a) and (c)). At the concentration ratios of 0.067, 0.127 and 0.201, the ohmic drop is low enough to avoid the onset of the current oscillations.

2.3. Potentiostatic current oscillations

Current oscillations were observed during the electrodeposition of Cd for a Cd^{2+}/CN^- concentration ratio above 0.254 (Fig. 19). The onset of oscillations with small amplitude was registered at -1.70 V (Fig. 19 (a)). At more positive potentials no current oscillations were observed. The amplitude of the oscillations increases with time, in the range between 2 mA cm^{-2} to 10 mA cm^{-2}. At a more negative potential, -1.75 V (Fig. 19 (b)), an increase of the range in the oscillation amplitude (50 mA cm^{-2} to 100 mA cm^{-2}), is observed.

Increasing the potential up to -1.80 V (Fig. 19 (c)), the oscillation amplitude reaches 120 mA cm^{-2}. At sufficient high potential (Fig. 19 (d)), the current oscillations live for a

short time. During potentiostatic electrodeposition, a simultaneous continuous hydrogen evolution was observed from the cathode surface with the naked eye. At a more negative potential the hydrogen evolution is faster. The current oscillations can be observed for hours under appropriately controlled conditions [88].

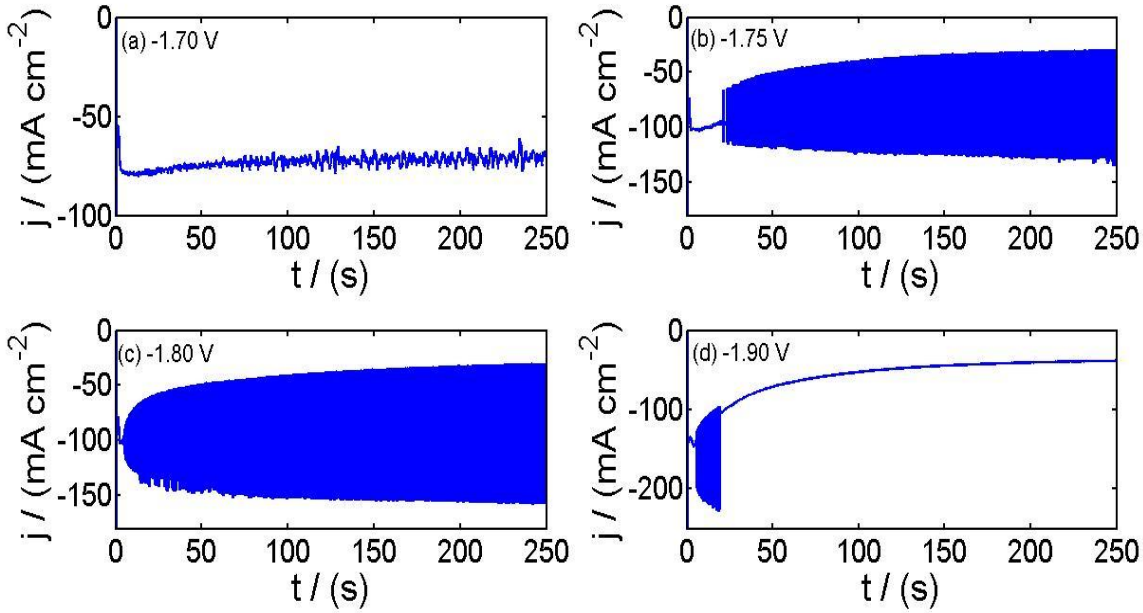

Fig. 19 Time series at different voltages registered during the electrodeposition of cadmium for a Cd^{2+}/CN^{-}= 0.254 concentration ratio at: (a) -1.70 V; (b) -1.75 V; (c) -1.80 V, and (d) -1.90 V.

It should be noted that even though there is continuous hydrogen evolution, the surface of the electrode is always covered by bubbles of hydrogen. The convection induced by the hydrogen evolution is always present, causing a continuous replenishment of the Cd concentration. The changes on the electrode surface, due to the adsorbed hydrogen bubbles on said surface and their continuous evolution, or the formation of some passive layer [70], could be the reason of the current oscillations.

Figures 20 and 21 show that current oscillations can be also registered at higher concentration ratios (0.268 and 0.334, respectively), and the higher the concentration ratio of the solution the higher the applied potential needed for the onset and cease of the current oscillations. In each case, continuous hydrogen evolution was observed with the naked eye. For the concentration ratio of 0.268 (Fig. 20), the current oscillations only were observed for a short time at the beginning of the experiments. At a Cd^{2+}/CN^{-}= 0.334 concentration ratio (Fig. 21), the oscillations appeared at the end of the experiments.

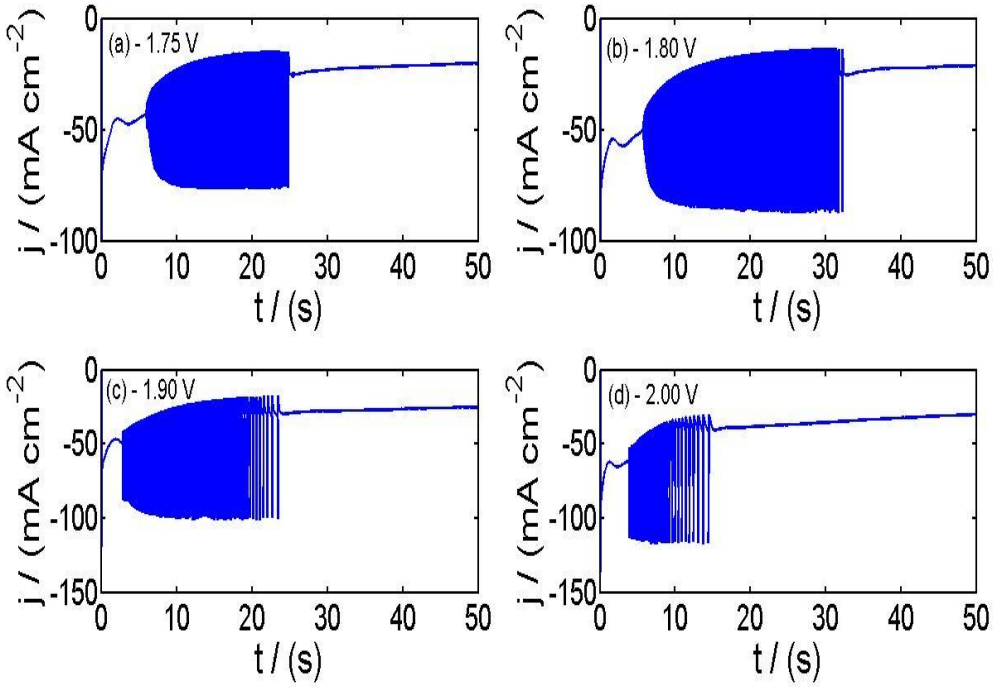

Fig. 20 Time series at different voltages registered during the electrodeposition of cadmium for a Cd^{2+}/CN^{-}= 0.268 concentration ratio at: (a) -1.75 V; (b) -1.80 V; (c) -1.90 V, and (d) -2.00 V.

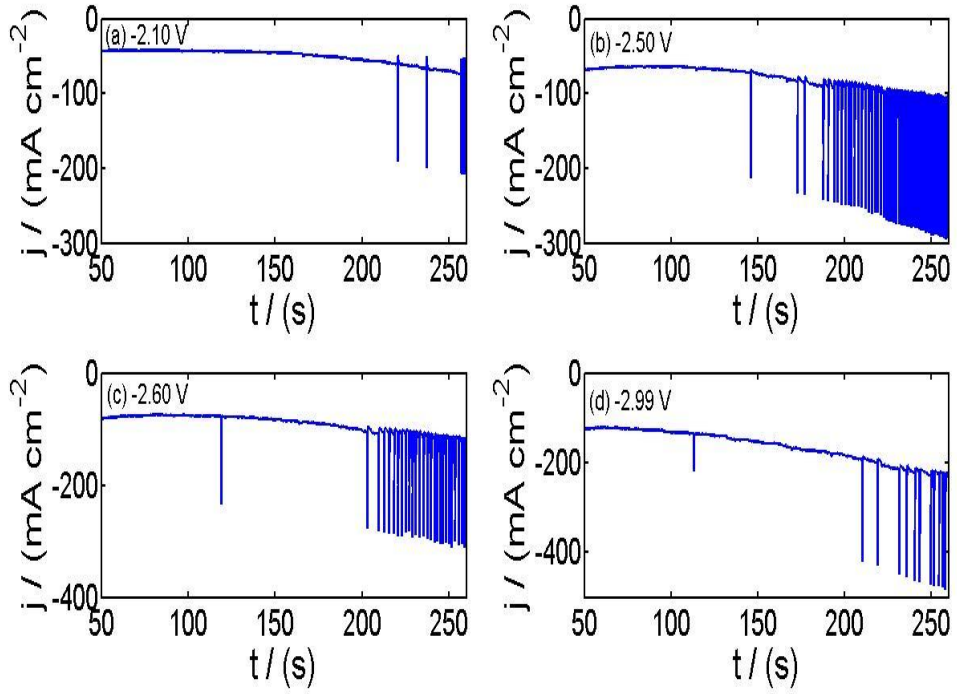

Fig. 21 Time series at different voltages registered during the electrodeposition of cadmium for a Cd^{2+}/CN^{-}= 0.334 concentration ratio at: (a) -2.10 V; (b) -2.50 V; (c) -2.60 V, and (d) -2.99 V.

Table II shows the range of potentials at which the current oscillations can be registered, at the different concentration ratios (Table I) studied in this work. It can be noted that under a potentiostatic condition it is necessary to apply a higher potential when the concentration ratio is increased, to observe current oscillations.

Table II. Range of potentials at which the current oscillations can be registered.

Concentration ratio	Range of potentials for current oscillations	
	V_i, (V)	V_f, (V)
0.067 (S1)	unobservable	
0.127 (S2)	unobservable	
0.201 (S3)	unobservable	
0.254 (S4)	-1.7	-1.9
0.268 (S5)	-1.75	-2
0.334 (S6)	-2.1	-2.99

Figure 22 ((a)-(c)) presents a zoomed time scale of the behaviour of the first three time series for a Cd^{2+}/CN^-= 0.254 concentration ratio (Fig. 19), and their respective Fourier Transforms (Fig. 22 (d)-(f)). At the lowest potential (Fig. 22 (a)), only broadened peaks with high noisy background can be observed (Fig. 22 (d)), which is characteristic of chaotic behaviour. For periodic or quasi-periodic behaviour, a sharp fundamental frequency and few harmonics can be clearly seen (Fig. 22 (e)-(f)). The frequency of the current oscillations diminishes with the increase in applied potential.

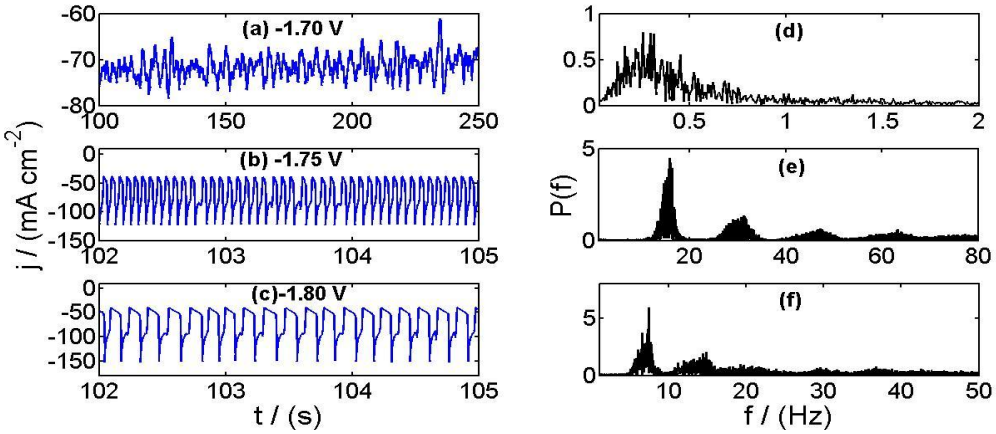

Fig. 22 Zoomed time scale of the behaviour of the current oscillations during the electrodeposition of Cd for a Cd^{2+}/CN^-= 0.254 concentration ratio at different potentiostatic conditions (a - c), and their corresponding Fast Fourier Transform spectra (d-f).

It can be noted that the oscillations (Fig. 23) show the same behaviour at different concentration ratios, as well as under different potentiostatic conditions. The FFT shows that the oscillations have quasiperiodic (Fig. 23 (f)) and chaotic features (Fig. 23 (d)-(e)).

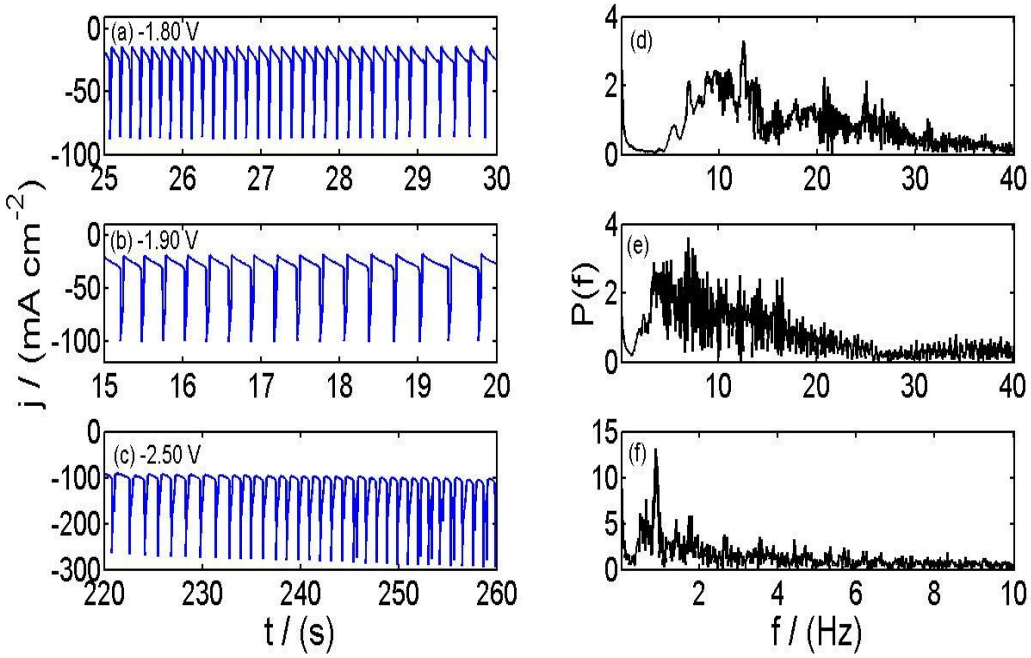

Fig. 23 Zoomed time scale of the behaviour of the current oscillations during the electrodeposition of Cd at different potentiostatic conditions for: (a) Cd^{2+}/CN^{-}= 0.268 at -1.80 V; (b) Cd^{2+}/CN^{-}= 0.268 at -1.90 V; (c) Cd^{2+}/CN^{-}= 0.334 at -2.50 V; and their corresponding Fast Fourier Transform spectra (d-f), respectively.

The two-dimensional phase portraits, done with the delay method, for the time series obtained for electrodeposition of Cd at potentiostatic conditions, are presented in Fig. 24. A strange attractor can be seen (Fig. 24 (a)), which means chaotic behaviour. A torus attractor, characteristic for quasi-periodic behaviour, is shown in Fig. 24 (b) and (d). Parts of the Fig. 24 (b) and (d) are zoomed in Fig. 24 (c) and (e), respectively, which show that two cycles of oscillations are present in the dynamical oscillatory behaviour. Those cycles, of small amplitude in the signal, correspond to those observed in Fig 22 (b) and (c). The broadened band in Fig. 24 (b), (d) appears because of a little variance in width and height of the oscillation peaks, due to the depletion of the reactants near the cathode during Cd electrodeposition.

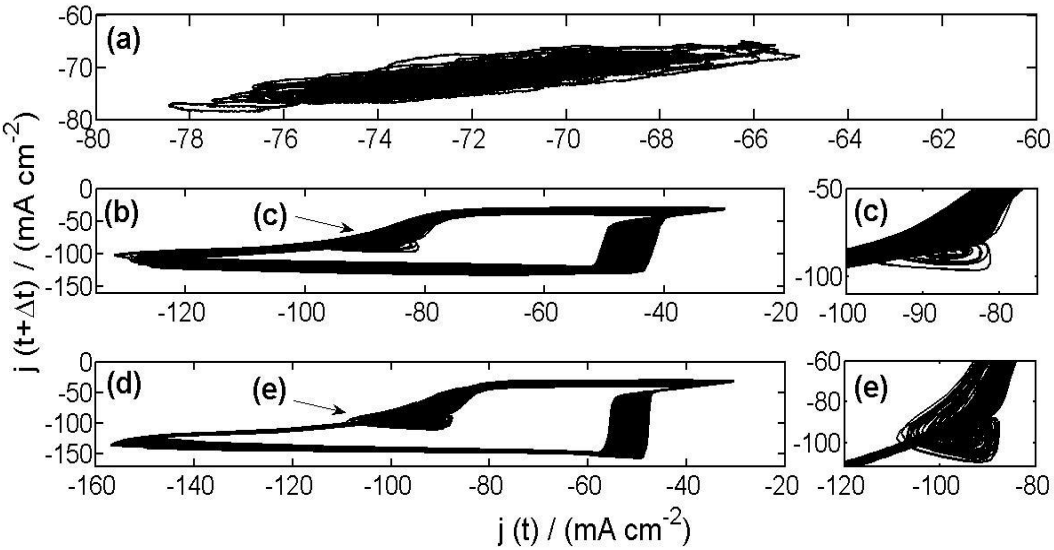

Fig. 24 Two-dimensional phase portraits of the time series obtained for the electrodeposition of Cd for a Cd^{2+}/CN^- concentration ratio of 0.264 at different potentials: (a) -1.70 V and Δt= 0.2 s, (b) -1.75 V and Δt= 0.005 s, (c) zoomed scale of the region appointed in (b), (d) -1.80 V and Δt= 0.005 s and (e) zoomed scale of the region appointed in (d).

As it can be noted the same behaviours are observed for the electrodeposition of Cd at different Cd^{2+}/CN^- concentration ratios and at different potentiostatic conditions. Strange attractors (Fig 25 (a) and (b)) represent chaotic behaviour. Figure 25 (c) (torus attractor) is characteristic for quasi-periodic behaviour.

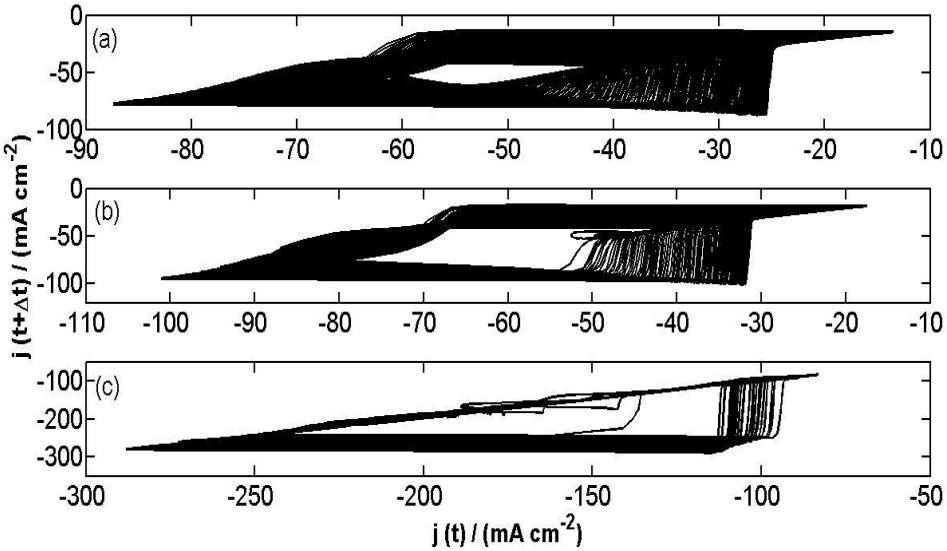

Fig. 25 Two-dimensional phase portraits of the time series obtained for the potentiostatic electrodeposition of Cd for: (a) Cd^{2+}/CN^-= 0.268 at -1.80 V and Δt= 0.005 s, (b) Cd^{2+}/CN^-= 0.268 at -1.90 V and Δt= 0.005 s, (c) Cd^{2+}/CN^-= 0.334 at -2.50 V and Δt= 0.005 s.

2.4. Galvanostatic potential oscillations

Potential oscillations were observed during the electrodeposition of Cd from a cyanide electrolyte. Figure 26 shows the conditions at which the onset of the cathodic potential oscillations occurred, at the different concentration ratios (Table I). It is necessary to apply a higher current density, for the onset of the potential oscillation, when the concentration ratio increases.

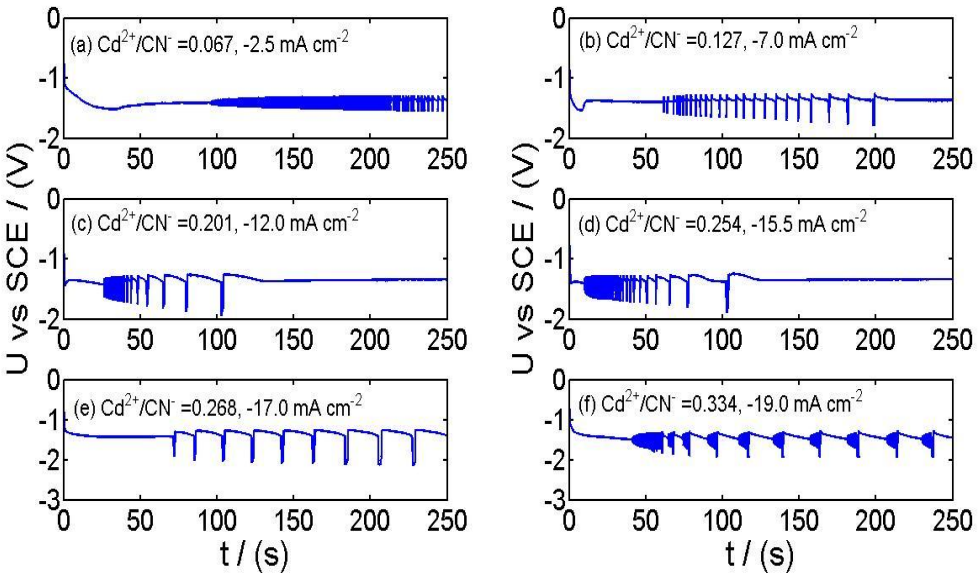

Fig. 26 Time series for the onset of the cathodic potential oscillations registered during the galvanostatic deposition of cadmium: (a) Cd^{2+}/CN^{-}= 0.067 at -2.5 mA cm^{-2}, (b) Cd^{2+}/CN^{-}= 0.127 at -7.0 mA cm^{-2}, (c) Cd^{2+}/CN^{-}= 0.201 at -12.0 mA cm^{-2}, (d) Cd^{2+}/CN^{-}= 0.254 at -15.5 mA cm^{-2}, (e) Cd^{2+}/CN^{-}= 0.268 at -17.0 mA cm^{-2} and (f) Cd^{2+}/CN^{-}= 0.334 at -19.0 mA cm^{-2}.

As an example, Figure 27 shows the dynamical behaviour during the galvanostatic electrodeposition of Cd from a Cd^{2+}/CN= 0.254 concentration ratio. At current densities lower than -15.5 mA cm^{-2} potential oscillations were not observed. Before the start of the oscillatory phase, different induction periods of several seconds are observed for the range of current densities between -15.5 mA cm^{-2} and -36.0 mA cm^{-2} (Figs. 27 (a)-(d)). At this point, the potential falls to more negative values. It can be seen that the increase of the current density causes a reduction in the induction period, as a consequence of the higher rate (current density) of the Cd electrodeposition process and hydrogen production. During the potential oscillations pulsating simultaneous hydrogen evolution was observed.

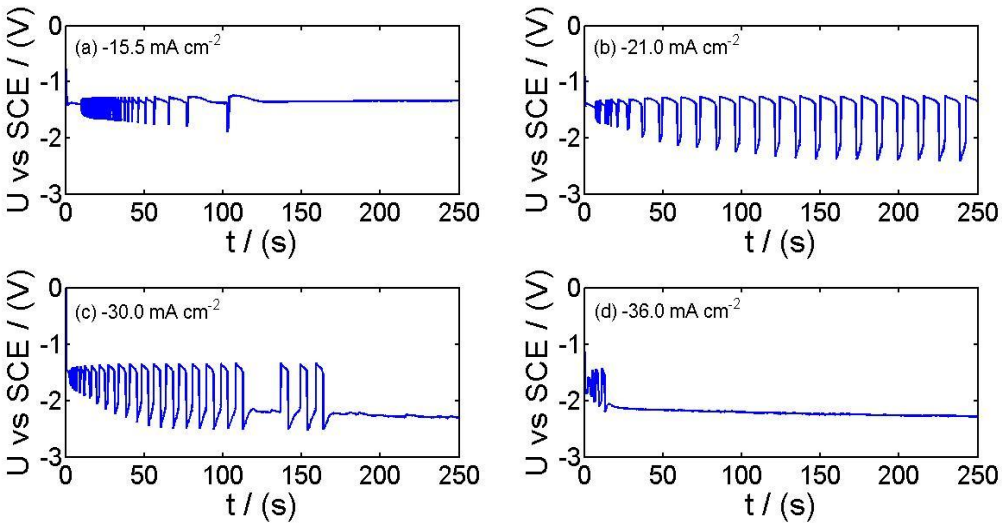

Fig. 27 Time series at different current densities registered during the cathodic galvanostatic deposition of Cd from a solution with a Cd^{2+}/CN^{-}= 0.254 concentration ratio: (a) -15.5 mA cm^{-2}; (b) -21.0 mA cm^{-2}; (c) -30.0 mA cm^{-2}; and (d) -36.0 mA cm^{-2}.

At the current density of -15.5 mA cm^{-2} (Fig. 27 (a)), the potential oscillations appear with an amplitude of about 300 mV, increasing in time up to 500 mV. At higher current densities the amplitude of the oscillations goes from 380 mV to 1100 mV (Figs. 27 (b)-(c)).

At a higher current density (-36.0 mA cm^{-2}, Fig. 27 (d)), the potential oscillations live for a short time, and they are no longer observable with the increase of current density. At this stage intensive hydrogen evolution occurs. The potential oscillations can be observed for a long time at the adequate conditions.

The cathodic potential fluctuations are characterized by an abrupt shift to more negative values, when hydrogen bubbles detach from the surface of the electrode, and then return immediately to less negative (noble) potential. At this point the electrode surface starts to be covered by hydrogen bubbles, diminishing the active surface area, and as a consequence the potential again tends slowly to more negatives values, followed by an abrupt shift to the most negative value, when the hydrogen bubbles detach, returning the cathodic potential to a less negative value, and so on.

The next five figures (Figs. 28-32) present some of the galvanostatic conditions, at which the potential oscillations were registered, for the different concentration ratios studied.

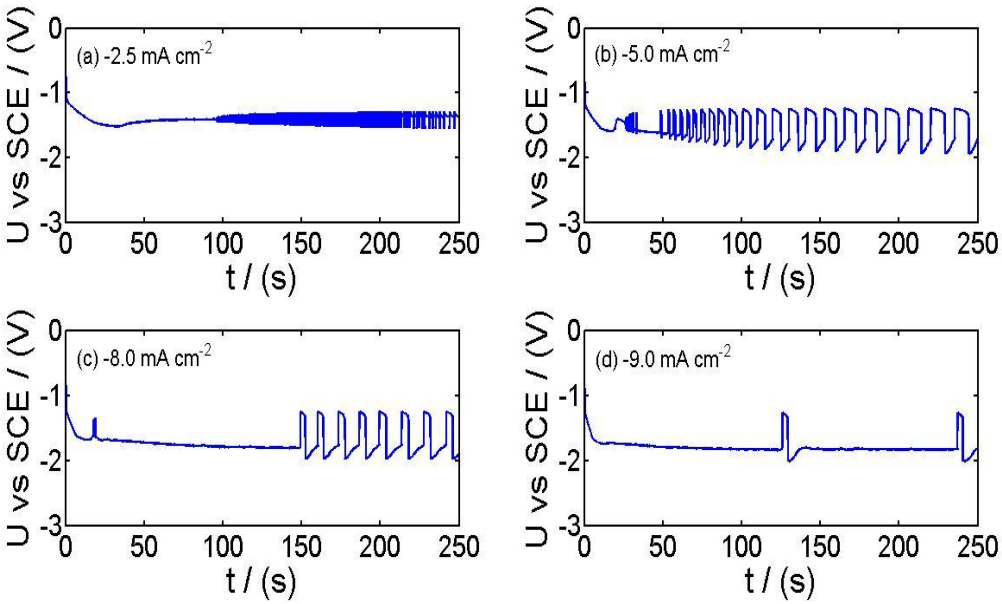

Fig. 28 Time series at different current densities registered during the cathodic galvanostatic deposition of Cd from a Cd^{2+}/CN^{-}= 0.067 concentration ratio: (a) -2.5 mA cm^{-2}; (b) -5.0 mA cm^{-2}; (c) -8.0 mA cm^{-2}; and (d) -9.0 mA cm^{-2}.

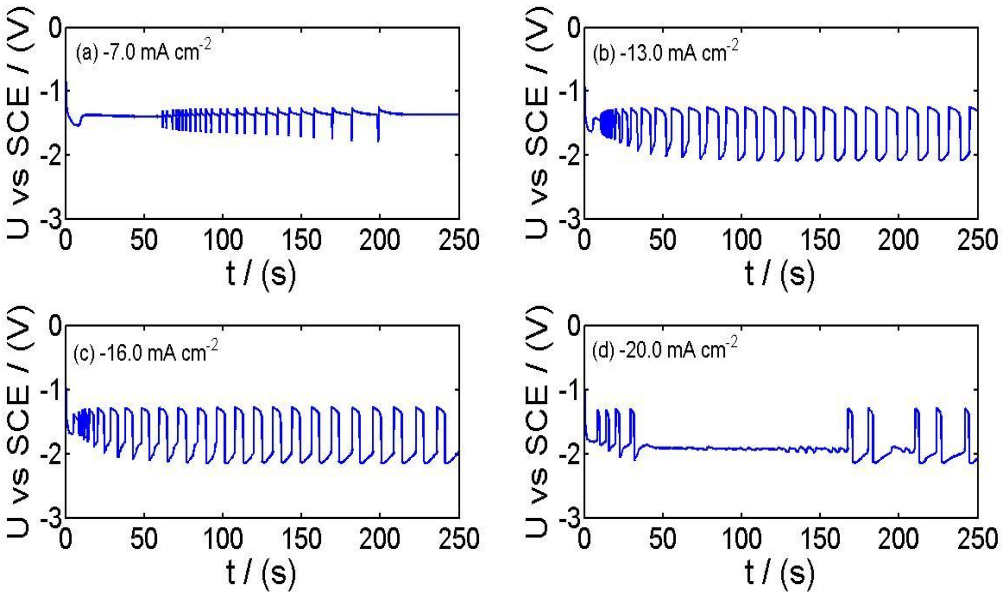

Fig. 29 Time series at different current densities registered during the cathodic galvanostatic deposition of Cd from a Cd^{2+}/CN^{-}= 0.127 concentration ratio: (a) -7.0 mA cm^{-2}; (b) -13.0 mA cm^{-2}; (c) -16.0 mA cm^{-2}; and (d) -20.0 mA cm^{-2}.

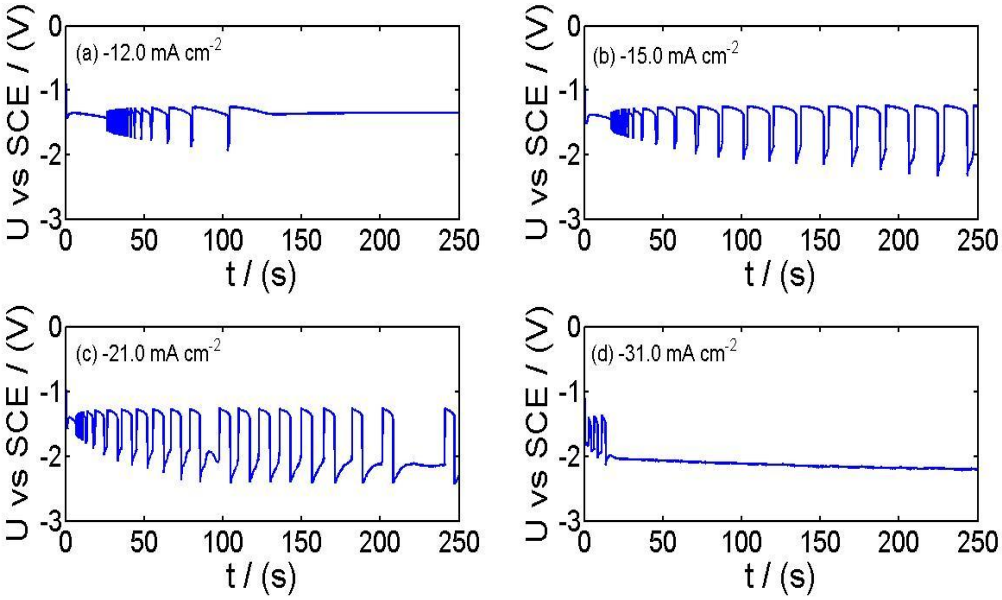

Fig. 30 Time series at different current densities registered during the cathodic galvanostatic deposition of Cd from a Cd^{2+}/CN^{-}= 0.201 concentration ratio: (a) -12.0 mA cm^{-2}; (b) -15.0 mA cm^{-2}; (c) -21.0 mA cm^{-2}; and (d) -31.0 mA cm^{-2}.

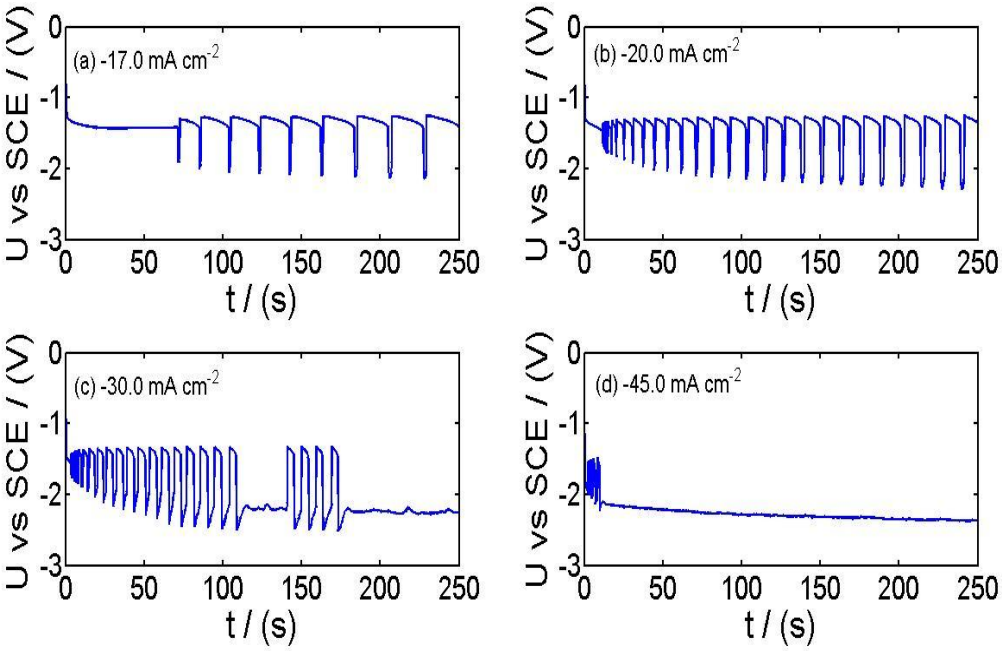

Fig. 31 Time series at different current densities registered during the cathodic galvanostatic deposition of Cd from a Cd^{2+}/CN^{-}= 0.268 concentration ratio: (a) -17.0 mA cm^{-2}; (b) -20.0 mA cm^{-2}; (c) -30.0 mA cm^{-2}; and (d) -45.0 mA cm^{-2}.

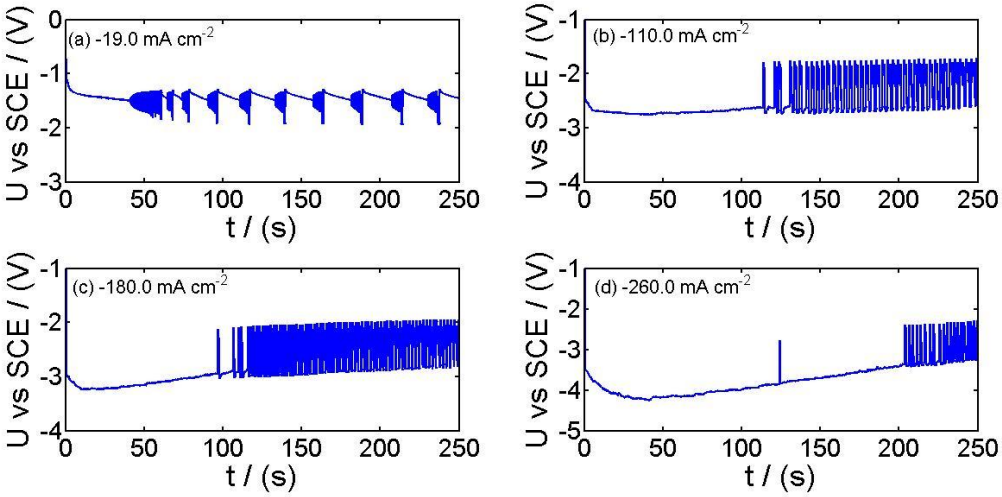

Fig. 32 Time series at different current densities registered during the cathodic galvanostatic deposition of Cd from a Cd^{2+}/CN^{-}= 0.334 concentration ratio: (a) -19.0 mA cm^{-2}; (b) -110 mA cm^{-2}; (c) -180.0 mA cm^{-2}; and (d) -260.0 mA cm^{-2}.

Table III shows the range of current densities at which the potential oscillations can be registered, at the different concentration ratios (Table I) studied in this work.

Table III. Range of current densities at which the potential oscillations can be registered.

Concentration ratio	Range of current densities for potential oscillations	
	j_i, (mA cm^{-2})	j_f, (mA cm-2)
0.067 (S1)	-2.5	-9.0
0.127 (S2)	-7.0	-20.0
0.201 (S3)	-12.0	-31.0
0.254 (S4)	-15.5	-39.0
0.268 (S5)	-17.0	-45.0
0.334 (S6)	-19.0	-260.0

Some of the times series obtained at galvanostatic conditions, were selected for the study of their dynamical features. Figures 33 ((a)-(d)) present a zoomed time scale of the potential oscillatory behaviour during galvanostatic conditions, and their respective Fourier Transforms (Fig. 33 (e)-(h)).

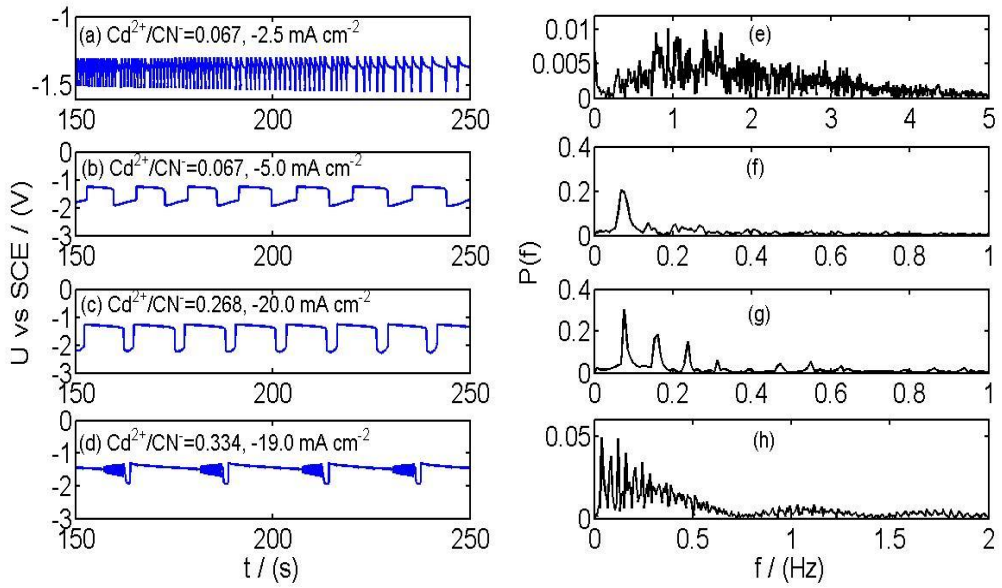

Fig. 33 Zoomed time scale of the potential oscillation behaviour during Cd electrodeposition at different current densities and concentration ratios: (a) Cd^{2+}/CN^{-}=0.067, -2.5 mA cm^{-2}; (b) Cd^{2+}/CN^{-}=0.067, -5.0 mA cm^{-2}; (c) Cd^{2+}/CN^{-}=0.268, -20 mA cm^{-2}; (d) Cd^{2+}/CN^{-}=0.334, -19 mA cm^{-2}, and their corresponding Fast Fourier Transform spectra (e-h).

Figure 33 presents different behaviours that can be registered when the Cd^{2+}/CN^{-} concentration ratio or current density is varied, during the electrodeposition of Cd. The lowest concentration ratio (Cd^{2+}/CN^{-}=0.067, Fig. 33 (a)), shows only broadened peaks with high noisy background in FFT (Fig. 33 (e), which is characteristic of chaotic behaviour. As well as for the potentiostatic current oscillations, a sharp fundamental frequency and a few harmonics are visible at some conditions (Figs. 33 (f)-(g)), representing periodic or quasi-periodic behaviour. The Fourier Transform (Fig. 33 (h)) of the highest concentration is characteristic of chaotic behaviour.

The two-dimensional phase portraits, constructed with the delay method, for the time series of Cd electrodeposition at galvanostatic conditions, are presented in Fig. 34. At the studied conditions torus attractors (fig. 34 (b) and (c)) were observed, characteristic for quasi-periodic behaviour.

The broadened band, similarly as in the case of potentiostatic current oscillations (Figs. 24, 25), appeared because of the variance in width and height of the oscillation peaks with time, due to of the depletion of the reactants in the electrochemical solution. Chaotic behaviour is represent by the strange attractors (Fig. 34 (a) and (d))

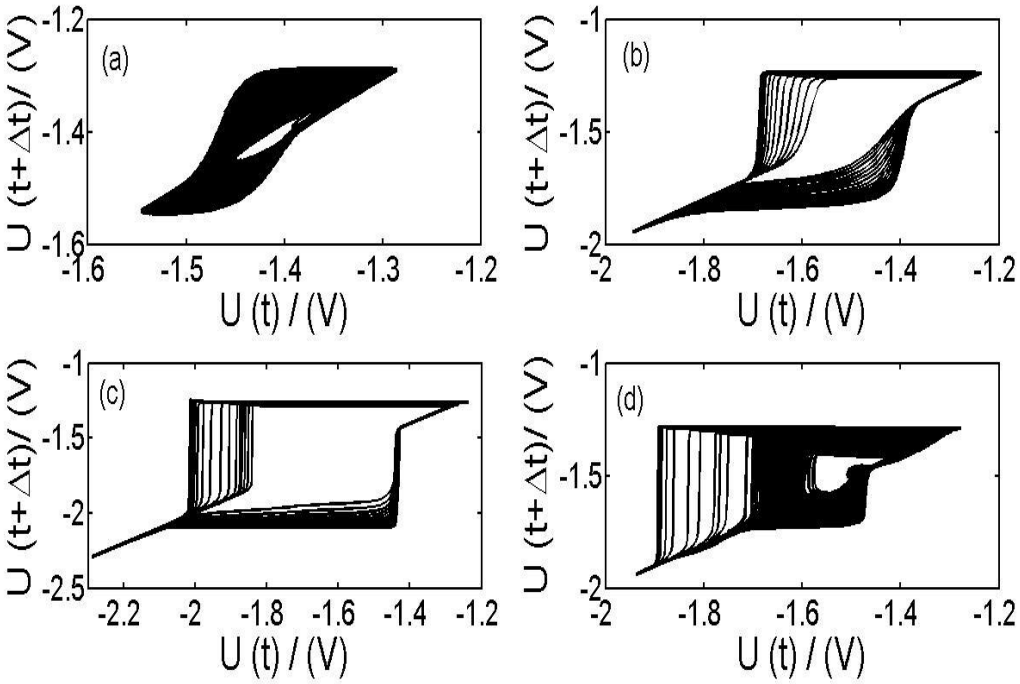

Fig. 34 Two-dimensional phase portraits of the time series of the galvanostatic electrodeposition of Cd for: (a) Cd^{2+}/CN^{-}=0.067 at -2.5 mA cm^{-2} and Δt= 0.02 s; (b) Cd^{2+}/CN^{-}=0.067 at -5 mA cm^{-2} and Δt= 0.01 s, (c) Cd^{2+}/CN^{-}=0.268 at -20 mA cm^{-2} and Δt= 0.01 s, (d) Cd^{2+}/CN^{-}=0.334 at -19 mA cm^{-2} and Δt= 0.01 s.

2.5. Surface morphology

Figure 35 shows representative SEM images of the surface morphology of the Cd electrodeposits, obtained under galvanostatic conditions for solutions with different concentrations ratios. The electrodeposited samples were obtained at the current densities where the onset and cease of the potential oscillations were registered. As it was mentioned above, when the concentration ratio of the solution increases, the current density necessary for the onset of oscillations is higher, as well as the current density for their cease. The SEM images show the formation of crystalline structures in block form or hexagonal plates, which exhibit preferential orientation in certain areas, depending on the conditions at which were obtained.

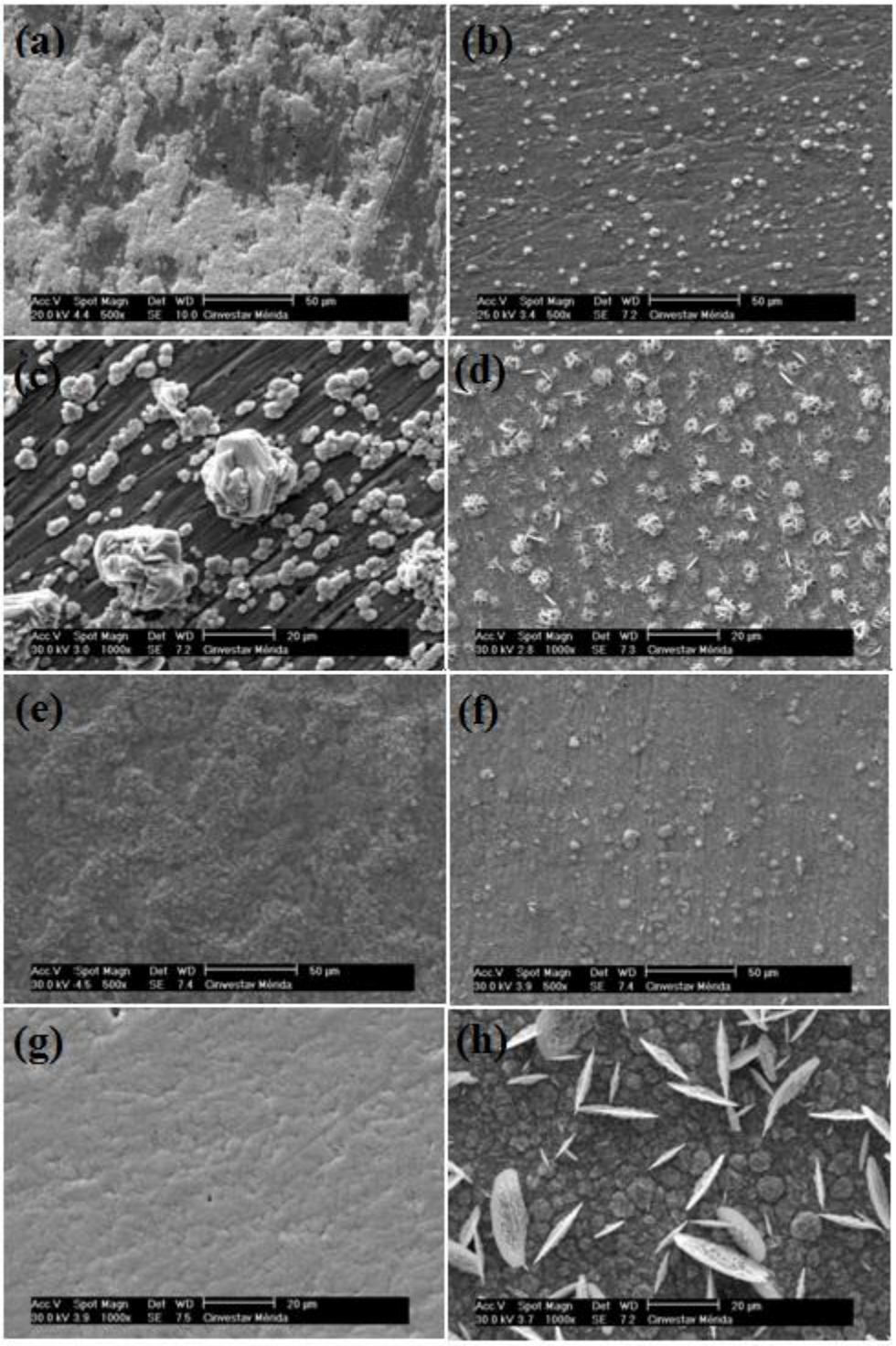

Fig. 35 SEM images of the coating surface for the electrodeposition of cadmium under galvanostatic conditions from solutions with a Cd^{2+}/CN^- concentration ratio: 0.127 (a)-7.0 mA cm^{-2}, (b)-20 mA cm^{-2}; 0.201 (c)-12 mA cm^{-2}, (d)-31 mA cm^{-2}; 0.268 (e)-17 mA cm^{-2}, (f)-45 mA cm^{-2}; 0.334 (g)-19 mA cm^{-2}, (h)-260 mA cm^{-2}.

The coatings obtained under potentiostatic conditions showed a sponge-like morphology (Fig. 36 (a), (c)) at the potential at which the onset of the current oscillations occurs, while at higher potentials (potential for the cease of the current oscillations), the morphology presents well-defined crystals of Cd covering the whole surface (Fig. 36 (b), (d)).

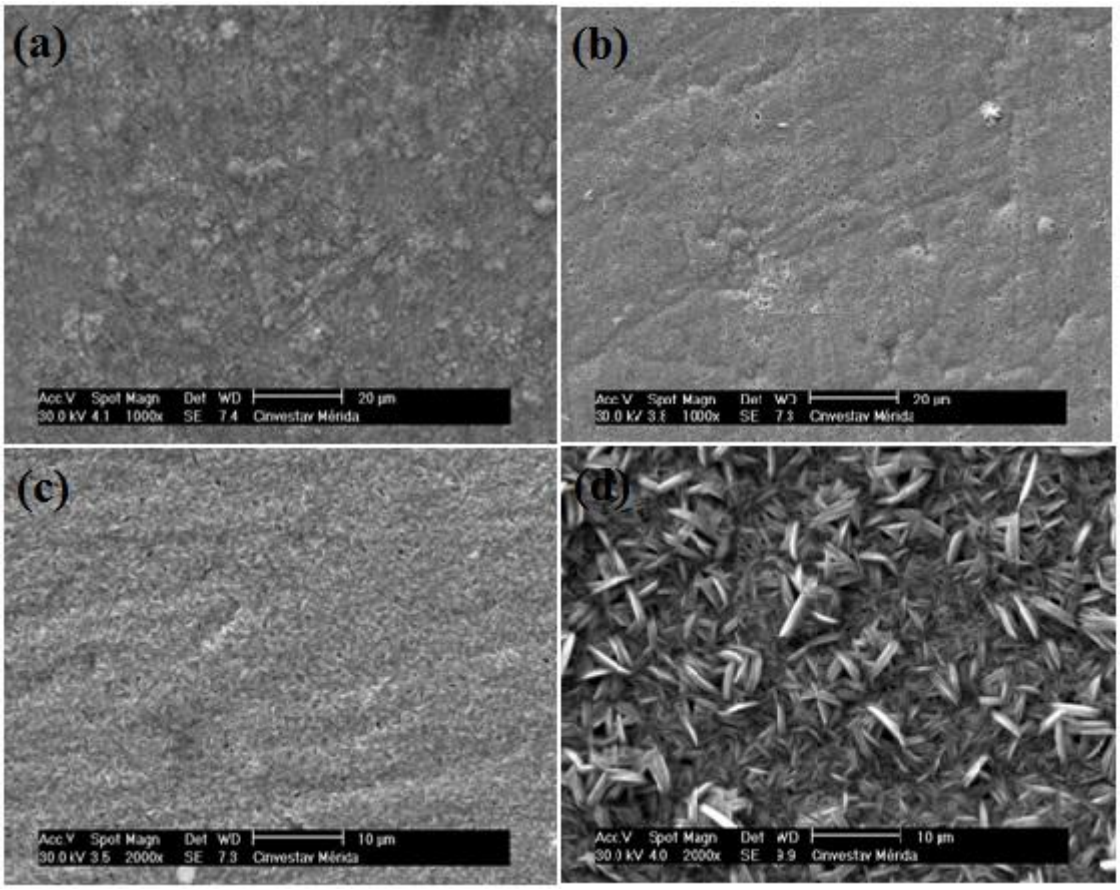

Fig. 36 SEM images of the coating surface for the electrodeposition of cadmium under potentiostatic conditions from solutions with a Cd^{2+}/CN^- concentration ratio: 0.268 (a) -1.75 V, (b)-2.00 V; 0.334 (c)-2.10 V, (d)-2.99 V.

2.6. Conclusions

Cathodic current and potential oscillations were observed during electrodeposition of Cd from a cyanide electrolyte on a vertical Pt electrode, under potentiostatic and galvanostatic control, respectively.

The current-potential curve showed a typical (N-Shape) behaviour of electrochemical oscillators, in which a broad limiting current plateau exists. In the current plateau of the current-potential curve, the EIS experiments revealed a region of negative real impedance in a range of non-zero frequencies. This fact suggests the presence of a hidden negative differential resistance under *dc* conditions. The existence of current and potential oscillations, and the hidden negative differential resistance, allowed us to classify the cadmium electrodeposition process as an HN-NDR oscillator.

The observed oscillations could be mainly attributed to the changes on the real active cathodic area, due to the adsorption of the hydrogen molecule. The hydrogen ion reduction is a simultaneous process, which occurs always during the observed oscillations, replenishing de Cd ion concentration at the metal-electrolyte interface.

FFT and two-dimensional phase portraits of the time series showed that the oscillations present quasi-periodic and chaotic behaviour, depending on the experimental conditions.

2.7. Perspectives

The complexity of the electrochemical behaviour makes the system an interesting subject for numerical simulations to reproduce the reported instabilities, and discuss in more detail the mechanisms of the oscillation occurrence in this system.

REFERENCES

[1] S. K. Scott, *Oscillations, waves, and chaos in chemical kinetics*, Oxford University Press, New York, 1994.

[2] H. Degn, *J. Chem. Educ.*, 1972, **49 (5)**, 302-307.

[3] I. R. Epstein, J. A. Pojman, *An introduction to nonlinear chemical dynamics: Oscillations, waves, patterns, and chaos*, ed. Oxford University Press, 3, 1998.

[4] I. R. Epstein, J. A. Pojman, O. Steinbock, *Chaos*, 2006, **16**, 037101- 037107.

[5] R. J. Field, E. Körös and R. M. Noyes, *J. Am. Chem. Soc.*, 1972, **94**, 8649-8664.

[6] R. J. Field, *J. Chem. Educ.*, 1972, **49 (5)**, 308-311.

[7] R. J. Field and F. W. Schneider, *J. Chem. Educ.*, 1989, **66 (3)**, 195-204.

[8] J. Happel and P. H. Sellers, *J. Phys. Chem*., 1991, **95**, 7740-7742.

[9] I. R. Epstein, *Physica D*, 1991, **51**, 152-155.

[10] G.T. Fechner, *Schweigger's J. Chemie. Physik*, 1828, **53**, 129-151.

[11] J. L. Hudson and T. T. Tsotsis, *Chem. Eng. Sci.*, 1994, **49**, 1493-1572.

[12] M.T. Gorzkowski, A. Wesolowska, R. Jurczakowski, P. Ślepski, K. Darowicki and M. Orlik, *J. Solid State Electrochem.*, 2011, **15**, 2311-2320.

[13] M.T. Gorzkowski and M. Orlik, *J. Solid State Electrochem.*, 2011, **15**, 2321-2330.

[14] G. A. Vázquez-Coutiño, M. Palomar-Pardavé, M. Romero-Romo, H. Herrera-Hernández and M. T. Ramírez-Silva, *Int. J. Electrochem. Sci., 2012*, **7**, 11641-11654.

[15] K. Schönleber and K. Krischer, *ChemPhysChem*, 2012, **13**, 2989-2996.

[16] I. Z. Kiss, L. N. Pelster, M. Wickramasinghe and G. S. Yablonsky, *Phys. Chem. Chem. Phys.*, 2009, **11**, 5720-5728.

[17] M. Pagitsas, D. Sazou, A. Karantonis and C. Georgolios, *J. Electroanal. Chem.*, 1992, **327**, 93-108.

[18] D. Sazou, A. Diamantopoulou and M. Pagitsas, *J. Electroanal. Chem.*, 2000, **489**, 1-16.

[19] R. Baba, Y. Shiomi and S. Nakabayashi, *Chem. Eng. Sci.*, 2000, **55**, 217-222.

[20] N. Cui, S. Zhao, C. Wang and S. Chen, *J. Serb. Chem. Soc.*, 2001, **66(8)**, 563-569.

[21] C. Wang, S. Chen and X. Yu, *Electrochim. Acta*, 1994, **39 (4)**, 577-580.

[22] Y. Zhai, I. Z. Kiss and L. Hudson, *Ind. Eng. Chem. Res.*, 2004, **43**, 315-326.

[23] S. Sadeghi and M. Thompson, *Phys. chem. chem. Phys.*, 2010, **12**, 6795-6809.

[24] Y. Xu and M. Schell, *J. Phys. Chem*., 1990, **94**, 7137-7143.

[25] M. F. Cabral, R. Nagao, E. Sitta, M. Eiswirth and H. Varela, *Phys. Chem. Chem. Phys.*, 2013, **15**, 1437-1442.

[26] M. Naito, H. Okamoto and N. Tanaka, *Phys. Chem. Chem. Phys.*, 2000, **2**, 1193-1198.

[27] J. Wojtowicz, N. Marincic and B. E. Conway, *J. Chem. Phys.*, 1968, **48**, 4333-4345.

[28] G. Baier, U. Kummer and S. Sahle, *J. Phys. Chem. A*, 1999, **103**, 33-37.

[29] Y. Mukouyama, S. Nakanishi, T. Chiba, K. Murakoshi and Y. Nakato, *J. Phys. Chem. B*, 2001, **105**, 7246-7253.

[30] Y. Mukouyama, S. Nakanishi, H. Konishi, Y. Ikeshima and Y. Nakato, *J. Phys. Chem. B*, 2001, **105**, 10905-10911.

[31] X.-C. Jiang, S. Chen, Z. Li, *Chin. J. Chem. Phys.*, 2006, **19 (3)**, 214-218.

[32] T. Tada, K. Fukami, S. Nakanishi, H. Yamasaki, S. Fukushima, T. Nagai, S.-I. Sakai and Y. Nakato, *Electrochim. Acta*, 2005, **50**, 5050-5055.

[33] E. W. Bohannan, L.-Y. Huang, F. S. Miller, M. G. Shumsky and J. A. Switzer, *Langmuir*, 1999, **15**, 813-818.

[34] J. Eskhult, M. Herranen and L. Nyholm, *J. Electroanal. Chem.*, 2006, **594**, 35-49.

[35] M.-Z. Zhang, M. Wang, Z. Zhang, J.-M. Zhu, R.-W. Peng and N.-B. Ming, *Electrochim. Acta*, 2004, **49**, 2379-2383.

[36] N. Kaneko, H. Nezu and N. Shinohara, *J. Electroanal. Chem.*, 1988, **252**, 371-381.

[37] Ts. Dobrovolska, I. Krastev and A. Zielonka, *ECS Transactions*, 2010, **25(20)**, 1-9.

[38] A. Bîrzu and V. Gáspár, *Electrochim. Acta*, 2009, **55**, 383-394.

[39] S. Schaltin, K. Binnemans and J. Fransaer, *Phys. Chem. Chem. Phys.*, 2011, **13**, 15448-15454.

[40] S. Kariuki, H. D. Dewald, J. Thomas and R. W. Rollins, *J. Electroanal. Chem.*, 2000, **486**, 175-180.

[41] S. Nakanishi, S.-I. Sakai, T. Nagai and Y. Nakato, *J. Phys. Chem. B*, 2005, **109**, 1750-1755.

[42] A. Survila, Z. Mockus and R. Juškėnas, *Electrochim. Acta*,1998, **43 (8)**, 909-914.

[43] E. Joanni, E. R. Gonzalez and H. Varela, *Quim. Nova*, 2008, **31 (6)**, 1444-1449.

[44] M. Eiswirth, A. Freund and J. Ross, in *Advances in Chemical Physics*, ed. I. Prigogine and S. A. Rice, John Wiley & Sons, Inc., New York, 1991, vol. 80, p. 127.

[45] M. H. Ghayesh, H. Farokhi and M. Amabili, *Int. J. Eng. Sci.*, 2013, **71**, 137-155.

[46] H. Okamoto, N. Tanaka and M. Naito, *Chem. Phys. Lett.*, 1995, **237**, 432-436.

[47] D. A. Hsieh, *J Financ.*, 1991, **46 (5)**, 1839-1877.

[48] M. T. M. Koper, in *Advances in Chemical Physics, ed. I. Prigogine and S. A. Rice*, John Wiley & Sons, Inc., New York, 1996, vol. 92, p. 161.

[49] Yu. A. Chizmadzhev and V. F. Pastushenko, in Comprehensive Treatise of Electrochemistry, ed by J. O' M. Bockris and R. E. White, Plenum Press, New York, 1995, **10**, p. 381.

[50] http://cordis.europa.eu/project/rcn/89037_en.html. Dynamo project of the European commission, *Design and functionality of nonlinear electrochemical nanoescale devices*, project reference no. 028669.

[51] M.T.M. Koper and J.H. Sluyters, *J. Electroanal. Chem.*, 1991, **303**, 65-72.

[52] M.T.M. Koper and J.H. Sluyters, *J. Electroanal. Chem.*, 1991, **303**, 73-94.

[53] M.T.M. Koper and J.H. Sluyters, *J. Electroanal. Chem.*, 1993, **352**, 51-64.

[54] M.T.M. Koper and J.H. Sluyters, *J. Electroanal. Chem.*, 1993, **347**, 31-48.

[55] M.T.M. Koper and J.H. Sluyters, *J. Electroanal. Chem.*, 1994, **371**, 149-159.

[56] W. Wolf, M. Lübke, M.T.M. Koper, K. Krischer, M. Eiswirth and G. Ertl, *J. Electroanal. Chem.*, 1995, **399**, 185-196.

[57] T.G.J. van Venrooij and M.T.M. Koper, *Electrochim. Acta.*, 1995, **40**, 1689-1696.

[58] M.T.M. Koper, *J. Chem. Soc., Faraday Trans.*, 1998, **94**(10), 1369-1378.

[59] P. Strasser, M. Lübke, C. Eickes and M. Eiswirth, *J. Electroanal. Chem.*, 1999, **462**, 19-33.

[60] M.T.M. Koper, *J. Electroanal. Chem.*, 1996, **409**, 175-182.

[61] P. Strasser, M. Eiswirth and M.T.M. Koper, *J. Electroanal. Chem.*, 1999, **478**, 50-66.

[62] M. Orlik, *Self-Organization in Electrochemical Systems*, ed. F. Scholz, Springer, Berlin Heidelberg, 2012, vol. 1.

[63] M. Orlik, *Self-Organization in Electrochemical Systems*, ed. F. Scholz, Springer, Berlin Heidelberg, 2012, vol. 2.

[64] Z. Li, J. Cai and S. Zhou, *J. Chem. Soc., Faraday Trans.*, 1997, **93**, 3519-3522.

[65] Z. Li, J. Cai and S. Zhou, *J. Electroanal. Chem.*, 1997, **432**, 111-116.

[66] Z. Li, J. Cai, S. Zhou, *J. Electroanal. Chem.*, 1997, **436**, 195-201.

[67] Z. Li, Y. Yu, H. Liao and S. Yao, *Chem. Lett.*, 2000, **4**, 330-331.

[68] Z. L. Li, Q.H. Yuan, B. Ren, X.M. Xiao, Y. Zeng and Z.Q. Tian, *Electrochem. Commun*, 2001, **3**, 654-658.

[69] R. M. Vishomirskis, Kinetika Electroosazhdenia Metallov iz Kompleksnih Elecktrolitov, Nauka, Moskva, 1969.

[70] Ts. Dobrovolska, D.A. López-Sauri, L. Veleva and I. Krastev, *Electrochim. Acta*, 2012, **79**, 162-169.

[71] M. T. M. Koper, Ver-uit-evenwicht verschijnselen in eletrochemische systemen: Instabiliteiten, Oscillaties en Chaos, Thesis.

[72] I. Prigogine, *Introduction to Thermodynamics of Irreversible Processes*, Wiley, New York (1961).

[73] I. Prigogine, *Self-organization in nonequilibrium systems*, Wiley-Interscience, from dissipative structures to order through fluctuations (1977).

[74] D.A. López-Sauri, *Fenómenos electroquímicos lejos del equilibrio: reacción de Belousov-Zhabotinsky y electrodepósito de aleaciones*, tesis, 2011.

[75] M. Orlik, *J. Solid State Electrochem*., 2009, **13**, 245-261.

[76] P. Strasser, *The electrochemical Society Interface*, 2000, 46-52.

[77] S. K. Scott,*Chemical Chaos*, Oxford University Press, Oxford, 1991.

[78] C. Gabrielli, *Identification of electrochemical processes by frequeny response analysis*, Solartron analytical, Technical report number 004/83, issue 3, 1998.

[79] K. Krischer, in *Modern aspects of electrochemistry*, Number 32, edited by B. E. Conway *et al.* Kluwer Academic/Plenum Publishers, New York, 1999.

[80] J. Wojtowicz, *Oscillatory behavior in electrochemical systems*, in: J. O'M. Bockris, B. Conway, R. E. White (Eds), Modern Aspects of Electrochemistry, Vol. 8, Butterworths, London, 1973, p. 47.

[81] J.-C. Roux, *Dynamical systems theory illustrated: chaoticbehaviour in the Belousov-Zhabotinsky reaction*, in: R. J. Field and L. Györgyi (Eds), Chaos in chemistry and biochemistry, World Scientific Publishing, Singapure, 1993, p. 21-44.

[82] S. H. Strogatz, *Nonlinear dynamics and chaos with applications to physics, biology, chemistry and engineering*, Westview Press, Cambridge, MA, 1994.

[83] M. T. M. Koper, P. Gaspard and J. H. Sluyters, *J. Chem. Phys.*, 1992, **97**, 8250-8260.

[84] M. T. M. Koper, P. Gaspard and J. H. Sluyters, *J. Chem. Phys.*, 1992, **96**, 5674-5675.

[85] S. Sadeghi and M. Thompson, *Phys. Chem. Chem. Phys.*, 2010, **12**, 6795-6809.

[86] D. A. López-Sauri, L. Veleva and G. Pérez, *Int. J. Elecrochem. Sci.*, 2014, **9**, 1102-1116.

[87] J. C. Roux, R. H. Simoyi and H. L. Swinney, *Physica D*, 1985, **16**, 285-240.

[88] D. A. López-Sauri, L. Veleva and G. Pérez-Ángel, *Phys. Chem. Chem. Phys.*, 2015, **17**, 22266-22271.

PUBLICATIONS

Parts of this study have been published in research journals, as listed below.

Ts. Dobrovolska, D.A. López-Sauri, L. Veleva and I. Krastev, Oscillations and spatio-temporal structures during electrodeposition of AgCd alloys, in *Electrochimica Acta*, 2012, **79**, 162-169.

D. A. López-Sauri, L. Veleva and G. Pérez, Analysis of nonlinear galvanostatic oscillations in Ag-Cd alloys Electrodeposition, in *International Journal of Electrochemical Science*, 2014, **9**, 1102-1116.

D. A. López-Sauri, L. Veleva and G. Pérez-Ángel, Potentiostatic current and galvanostatic potential oscillations during electrodeposition of cadmium, in *Physical Chemistry Chemical Physics*, 2015, **17**, 22266-22271.